



HAL
open science

Over-calcified forms of the coccolithophore *Emiliana huxleyi* in high-CO₂ waters are not preadapted to ocean acidification

Peter von Dassow, Francisco Díaz-Rosas, El Mahdi Bendif, Juan-Diego Gaitán-Espitia, Daniella Mella-Flores, Sebastian Rokitta, Uwe John, Rodrigo Torres

► To cite this version:

Peter von Dassow, Francisco Díaz-Rosas, El Mahdi Bendif, Juan-Diego Gaitán-Espitia, Daniella Mella-Flores, et al.. Over-calcified forms of the coccolithophore *Emiliana huxleyi* in high-CO₂ waters are not preadapted to ocean acidification . Biogeosciences, 2018, 15 (5), pp.1515-1534. 10.5194/bg-15-1515-2018 . hal-01758791

HAL Id: hal-01758791

<https://hal.sorbonne-universite.fr/hal-01758791>

Submitted on 4 Apr 2018

HAL is a multi-disciplinary open access archive for the deposit and dissemination of scientific research documents, whether they are published or not. The documents may come from teaching and research institutions in France or abroad, or from public or private research centers.

L'archive ouverte pluridisciplinaire **HAL**, est destinée au dépôt et à la diffusion de documents scientifiques de niveau recherche, publiés ou non, émanant des établissements d'enseignement et de recherche français ou étrangers, des laboratoires publics ou privés.



Over-calcified forms of the coccolithophore *Emiliana huxleyi* in high-CO₂ waters are not preadapted to ocean acidification

Peter von Dassow^{1,2,3}, Francisco Díaz-Rosas^{1,2}, El Mahdi Bendif⁴, Juan-Diego Gaitán-Espitia⁵, Daniella Mella-Flores¹, Sebastian Rokitta⁶, Uwe John^{6,7}, and Rodrigo Torres^{8,9}

¹Facultad de Ciencias Biológicas, Pontificia Universidad Católica de Chile, Santiago, Chile

²Instituto Milenio de Oceanografía de Chile, Concepción, Chile

³UMI 3614 Evolutionary Biology and Ecology of Algae, CNRS, Sorbonne Université, Pontificia Universidad Católica de Chile, Universidad Austral de Chile, Station Biologique de Roscoff, 29680 Roscoff, France

⁴Department of Plant Sciences, University of Oxford, OX1 3RB Oxford, UK

⁵CSIRO Oceans and Atmosphere, G.P.O. Box 1538, Hobart 7001, TAS, Australia

⁶Alfred Wegener Institute – Helmholtz Centre for Polar and Marine Research, Bremerhaven, Germany

⁷Helmholtz Institute for Functional Marine Biodiversity (HIFMB), Ammerländer Heerstr. 231, 26129 Oldenburg, Germany

⁸Centro de Investigación en Ecosistemas de la Patagonia (CIEP), Coyhaique, Chile

⁹Centro de Investigación: Dinámica de Ecosistemas marinos de Altas Latitudes (IDEAL), Punta Arenas, Chile

Correspondence: Peter von Dassow (pvondassow@bio.puc.cl)

Received: 18 July 2017 – Discussion started: 6 September 2017

Revised: 25 January 2018 – Accepted: 7 February 2018 – Published: 14 March 2018

Abstract. Marine multicellular organisms inhabiting waters with natural high fluctuations in pH appear more tolerant to acidification than conspecifics occurring in nearby stable waters, suggesting that environments of fluctuating pH hold genetic reservoirs for adaptation of key groups to ocean acidification (OA). The abundant and cosmopolitan calcifying phytoplankton *Emiliana huxleyi* exhibits a range of morphotypes with varying degrees of coccolith mineralization. We show that *E. huxleyi* populations in the naturally acidified upwelling waters of the eastern South Pacific, where pH drops below 7.8 as is predicted for the global surface ocean by the year 2100, are dominated by exceptionally over-calcified morphotypes whose distal coccolith shield can be almost solid calcite. Shifts in morphotype composition of *E. huxleyi* populations correlate with changes in carbonate system parameters. We tested if these correlations indicate that the hyper-calcified morphotype is adapted to OA. In experimental exposures to present-day vs. future $p\text{CO}_2$ (400 vs. 1200 μatm), the over-calcified morphotypes showed the same growth inhibition ($-29.1 \pm 6.3\%$) as moderately calcified morphotypes isolated from non-acidified water ($-30.7 \pm$

8.8 %). Under the high-CO₂–low-pH condition, production rates of particulate organic carbon (POC) increased, while production rates of particulate inorganic carbon (PIC) were maintained or decreased slightly (but not significantly), leading to lowered PIC / POC ratios in all strains. There were no consistent correlations of response intensity with strain origin. The high-CO₂–low-pH condition affected coccolith morphology equally or more strongly in over-calcified strains compared to moderately calcified strains. High-CO₂–low-pH conditions appear not to directly select for exceptionally over-calcified morphotypes over other morphotypes, but perhaps indirectly by ecologically correlated factors. More generally, these results suggest that oceanic planktonic microorganisms, despite their rapid turnover and large population sizes, do not necessarily exhibit adaptations to naturally high-CO₂ upwellings, and this ubiquitous coccolithophore may be near the limit of its capacity to adapt to ongoing ocean acidification.

1 Introduction

Coccolithophores are planktonic single-celled photoautotrophs mostly in the range of 3–20 μm and characterized by bearing calcite plates (coccoliths) (Monteiro et al., 2016) and represent one of the most abundant and widespread groups of marine eukaryotic phytoplankton (Iglesias-Rodríguez et al., 2002; Litchman et al., 2015). In addition to being important primary producers, coccolithophores contribute most of the calcium carbonate (CaCO_3) precipitation in pelagic systems. Although CaCO_3 precipitation in the surface is a source of CO_2 , i.e., the “carbonate counter pump” (Frankignoulle et al., 1994), CaCO_3 may enhance sinking of organic matter by imposing a ballast effect on sinking aggregates (Armstrong et al., 2002; Sanders et al., 2010). Thus, this plankton functional group has a complex role in ocean carbon cycles. Roughly a third of current anthropogenic CO_2 emissions are being absorbed in the ocean (Sabine et al., 2004), driving a decrease in pH, the conversion of CO_3^{2-} to HCO_3^- , and a drop in saturation states of the CaCO_3 minerals aragonite and calcite (Ω_{Ar} , Ω_{Ca}), phenomena collectively termed ocean acidification (OA; Orr et al., 2005). Although most surface waters are expected to remain supersaturated with respect to calcite ($\Omega_{\text{Ca}} > 1$), which is less soluble than aragonite, the drop in Ω_{Ca} might still result in decreases in calcite biomineralization (Hofmann and Schellnhuber, 2009). Understanding the response of coccolithophores to OA is thus needed for predicting how pelagic ecosystems and the relative intensity of the biological carbon pumps will change as atmospheric CO_2 continues to increase.

Many studies designed to assess coccolithophores' responses to low pH have been performed in short-term culture and mesocosm experiments on timescales of weeks to months, and carbonate systems were usually manipulated to mimic preindustrial, present, and future CO_2 levels. Mesocosm studies have shown that North Sea populations of the cosmopolitan and abundant species *Emiliana huxleyi* are negatively impacted by low-pH conditions (Engel et al., 2005; Riebesell et al., 2017). However, a wide range of growth, calcification (particulate inorganic carbon, PIC), and productivity (particulate organic carbon, POC) responses to high- CO_2 –low-pH conditions have been reported in laboratory cultures of *E. huxleyi*, mostly using different regional strains (Riebesell et al., 2000; Iglesias-Rodríguez et al., 2008; Langer et al., 2009; Müller et al., 2015a, 2017; Olson et al., 2017; Jin et al., 2017). According to a recent comprehensive review and meta-analysis (Meyer and Riebesell, 2015), the mean responses of *E. huxleyi* averaged over 19 studies indicated that high- CO_2 –low-pH conditions have a negative effect on PIC quotas and production rates as well as PIC / POC ratios but no consistent effects on POC quotas and production rates. The response variability among strains of *E. huxleyi* (Langer et al., 2009; Müller et al., 2015a) is also seen within the genus *Calcidiscus* (Diner et al., 2015) and suggests a high potential for genetic adaptation within coccolithophores.

Such adaptive capacity to high- CO_2 –low-pH conditions has been suggested for *E. huxleyi* in long-term lab-based experimental evolution studies (up to 2000 generations) on clonal strains (Lohbeck et al., 2012; Schlüter et al., 2016). It is still difficult to know to which extent such experiments reflect real-world adaptation processes. First, only asexually propagating cells have yet been explored in the lab, while sexual recombination in natural populations is expected to accelerate adaptation (McDonald et al., 2016). Second, calcification is costly and in nature must be maintained by providing benefits to the cell. What these benefits are remains unclear. It has been suggested that coccoliths may provide defense against grazing or parasites and modify light–UV levels reaching the cell, amongst other proposed functions (Monteiro et al., 2016). The benefits of calcification likely vary among species and may have changed over the course of evolution or with environmental change. For example, in paleo-oceans, it might have helped alleviate toxicity from Ca^{2+} when levels reached up to 4-fold higher than in the modern ocean during the Cretaceous (Müller et al., 2015b). The long-term and nonlinear declines in calcification observed in experimental adaptation to high CO_2 and low pH (Schlüter et al., 2016) thus might have a high potential cost if such changes occurred in nature.

Complementary to experimental approaches, observational studies that correlate coccolithophore communities and levels or rates of calcification with variability in carbonate system parameters offer important insights into possible adaptations to high CO_2 and low pH. Focusing only on *E. huxleyi* and the closely related genus *Gephyrocapsa* (both within the family Noelaerhabdaceae), a general pattern has been documented of a decreasing calcite mass of coccoliths and coccospheres with increasing $p\text{CO}_2$ for both modern and recent fossil coccolithophores across the world's ocean basins (Beaufort et al., 2011). This pattern involved shifts away from more heavily calcified *Gephyrocapsa* that dominated assemblages under the lowest $p\text{CO}_2$ towards a spectrum of *E. huxleyi* morphotypes that were more abundant under intermediate and high $p\text{CO}_2$: *E. huxleyi* “type A” morphotypes with heavier coccoliths (more calcite per coccolith) dominated *E. huxleyi* populations in waters with intermediate $p\text{CO}_2$ while “type B/C” or “type C” morphotypes with successively lighter coccoliths dominated in higher- $p\text{CO}_2$ waters (Beaufort et al., 2011; Poulton et al., 2011).

Beyond this comparably clear pattern, the survey by Beaufort et al. (2011) also reported one important exception to the general trend: at two sites approaching the Chilean upwelling zone, forms of *E. huxleyi* with exceptionally over-calcified coccoliths dominated in naturally acidified upwelling waters, where $p\text{CO}_2$ reaches values more than 2-fold higher than the equilibrium with present-day atmospheric levels. Similarly, a year-long monthly survey of coccolithophore communities in the Bay of Biscay found that an over-calcified type A form dominated during the winter, when $p\text{CO}_2$ was highest, but contributed only a minor part to the *E. huxleyi* populations in

summer, when $p\text{CO}_2$ was lowest (Smith et al., 2012). One explanation might be that over-calcified morphotypes are especially tolerant to such ocean acidification (OA) conditions.

The eastern South Pacific off the coast of Chile and Peru presents a natural laboratory for investigating such hypotheses regarding organisms' responses to ocean acidification. The coastal zone is naturally acidified, with surface waters frequently reaching $p\text{CO}_2$ levels $> 1000 \mu\text{atm}$ and pH values < 7.7 during upwelling events (Friederich et al., 2008; Torres et al., 2011).

In this study, we surveyed the coccolithophore communities of the Chilean upwelling zone as well as adjacent coastal and offshore waters with varying $p\text{CO}_2$ levels and isolated *E. huxleyi* strains of dominant morphotypes. In lab-based experiments, three strains showing distinct over-calcification were compared with two moderately calcified type A morphotypes in terms of their response to altered CO_2 and pH (400 vs. $1200 \mu\text{atm}$ $p\text{CO}_2$) to investigate whether CO_2 might indeed be the environmental driver selecting for the extreme over-calcified morphotypes specific to the Chilean coast.

2 Materials and methods

2.1 Surveys

An oceanographic cruise (NBP 1305) was conducted onboard R/V *Nathaniel B. Palmer* (NBP) during the early austral winter (27 June–22 July 2013) along a transitional zone from coastal to open ocean waters off central-southern Peru and northern Chile (Fig. 1a). A total of 24 stations were sampled between 22 and 13° S and from 70 to 86° W (ranging from 47 to 1424 km from the coast). Central Chile coastal surveys were conducted onboard the R/V *Stella Maris II* (Universidad Católica de Norte) during the mid-spring of 2011 (12 October) and 2012 (28 November) and aboard a rented fishing launch (18–19 November 2012) in the high- $p\text{CO}_2$ upwelling zone in front of Tongoy Bay (TON), northern Chile ($\sim 30^\circ$ S– 72° W; Fig. 1b). These two coastal surveys consisted of seven sampling points distributed between 1 and 23 km off the coast. Another coastal sampling was conducted from a small launch (belonging to the Pontificia Universidad Católica de Chile) during the mid-spring of 2012 (10 November), in the upwelling zone in front of El Quisco Bay (QUI $\sim 33^\circ$ S– 72° W; Fig. 1b). This coastal survey consisted of one sampling point located 4 km offshore. Finally, one sampling was conducted from a rented fishing vessel during the mid-spring of 2011 (1 November), in the mesotrophic waters that surround the Juan Fernández Islands (JF; $\sim 33^\circ$ S– 78° W; Fig. 1b).

2.2 Physical–chemical oceanographic parameters

During the NBP cruise, temperature and salinity were measured with a SBE 25 CTD (Sea-Bird Scientific, Bellevue, WA, USA) from rosette casts or from the onboard running seawater system equipped with a SBE 45 conductivity sensor and a SBE 38 temperature sensor (both from Sea-Bird Scientific). During the 2011 cruise on the R/V *Stella Maris II*, an SBE 19 plus CTD was used (data courtesy of Beatriz Yannicelli). In other samplings, an SBE 18 plus CTD was used for water column measurements. On the 29 November 2012 cruise on the R/V *Stella Maris II*, surface samples were pumped continuously onboard in underway sampling and analyzed with a YSI Pro30 salinometer and thermometer (YSI, Yellow Springs, OH, USA).

In October 2011 and November 2012, duplicate 500 mL samples of surface seawater were collected into borosilicate bottles, fixed with $50 \mu\text{L}$ of HgCl_2 saturated solution, and stored until measurements of total dissolved inorganic carbon (DIC) and total alkalinity (TA). TA was determined using potentiometric titration in an open cell (Heraldsson et al., 1997). Standardization was performed and the accuracy was controlled against a certified reference material (CRM Batch 115 bottled in September 2011) supplied by Andrew Dickson (Scripps Institution of Oceanography, https://www.nodc.noaa.gov/ocads/oceans/Dickson_CRM/batches.html, Dickson, 2010). The correction factor was approximately 1.002. Precision (variation among replicas) in TA was always less than 0.5 % (average 0.1 %). DIC was determined using a fully automatic DIC analyzer (model AS-C3, Apollo SciTech, Newark, DE, USA), with variation among replicates averaging 0.1 % (max. 0.3 %). All the dissolved carbonate species from a seawater sample were extracted as CO_2 gas through acidification and nitrogen stripping. The CO_2 gas was then quantitatively detected with an infrared LI-7000 CO_2 analyzer (LI-COR Environmental, Lincoln, Nebraska USA). During the expedition off Juan Fernández (November 2011) pH and TA were measured in fixed samples. The pH was measured on the total ion scale using spectrophotometric detection of m-cresol purple absorption in a 100 mm quartz cell thermally stabilized at 25.0°C (Dickson et al., 2007) with a BioSpec 1600 spectrophotometer (Shimadzu Scientific Instruments, Kyoto, Japan), with pH among replicas varying less than 0.01 units. During the NBP cruise, direct measurements of sea surface $p\text{CO}_2$ using nondispersive infrared detection were obtained from continuous measurements by the Research Vessel Data Acquisition System (RVDAS; Lamont-Doherty Earth Observatory, Columbia University) in addition to TA samples.

Saturation states of aragonite (Ω_{Ar}) as well as calcite (Ω_{Ca}) and other carbonate system parameters were estimated from the DIC–TA pairs (for samplings off the central Chilean coast in October 2011 and November 2012), pH–TA (for expedition off the Juan Fernández Islands in November 2011),

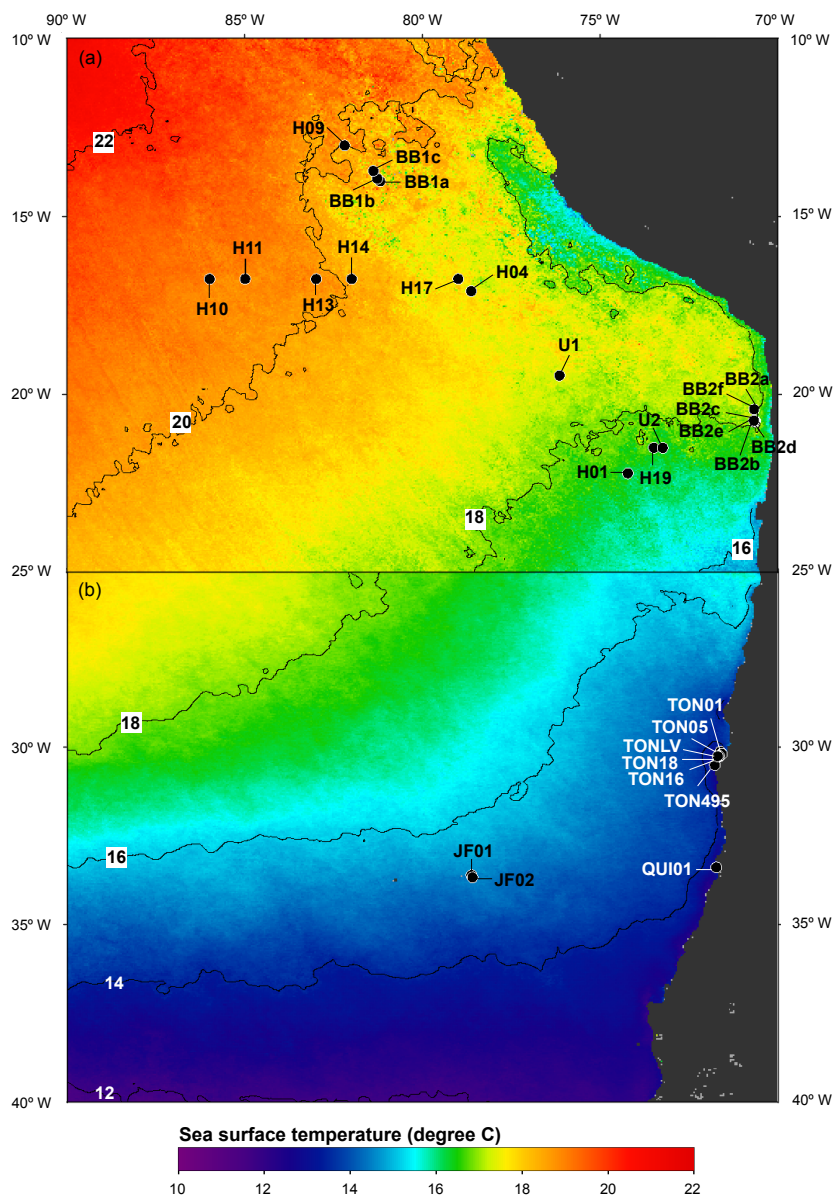


Figure 1. Map of stations sampled during the NBP 1305 cruise (June–July 2013) (a) and in smaller field expeditions of October–November in 2011–2012 (b). Sea surface temperature climatologies (2002–2012) are plotted for the months of July (a) and October (b).

and $p\text{CO}_2$ –TA pairs (for the NBP 1305 cruise during June–July 2013) using CO2SYS software (Pierrot et al., 2006) set with Mehrbach solubility constants (Mehrbach et al., 1973) refitted by Dickson and Millero (Dickson and Millero, 1987). Environmental parameters are provided in Table S1.

Mean sea surface temperature and chlorophyll *a* (chl *a*) monthly climatologies (2002–2014) were obtained from the MODIS-Aqua satellite (NASA Goddard Space Flight Center, Ocean Ecology Laboratory, and Ocean Biology Processing Group, 2014) and plotted using SeaDAS (Baith et al., 2001) version 7.1 for Mac OS X.

2.3 Phytoplankton analyses

Discrete seawater samples (Niskin bottles) containing planktonic assemblages were collected at various depths within the upper 150 m, depending on depth of the maximum chl *a* fluorescence (as proxy of phytoplankton) and from the onboard seawater system when Niskin samples were not available. Duplicate 100 mL samples of seawater (previously filtered through 200 μm Nitex mesh) were fixed (final concentration 1 % formaldehyde, 0.05 % glutaraldehyde, and 10 mM borate pH 8.5) and stored at 4 °C until light microscopic examination.

Samples were sedimented in 100 mL Utermöhl chambers for 48 h prior to counting. The absolute abundance of microplankton (20–200 μm in size) and coccolithophores (ranging from 2.5 to 20 μm in size, but mostly comprised of species within the range of 3–10 μm including *E. huxleyi*, several species of the genera *Gephyrocapsa*, and *Calcidiscus leptoporus*) were estimated with an inverted microscope (Olympus CKX41) connected to a digital camera (Motic 5.0). For counts of large diatoms, thecate dinoflagellates, and other planktonic cells (> 50 μm in size), a 20 \times objective was used. For counts of small diatoms and atecate dinoflagellates (< 50 μm in size) a 40 \times objective was used. For counts of total coccolithophores, a 40 \times objective was used with cross-polarized light (Edmund Optics polarizers 54 926 and 53 347).

In parallel, duplicate 250 mL samples of seawater were filtered onto polycarbonate filters (0.2 μm pore size; Millipore), which were dried and stored in petri dishes until processing for identification of coccolithophore species and *E. huxleyi* morphotypes. A small cut portion of each dried filter was sputter-coated with gold. The identification and relative abundance of coccolithophore species was performed by counting a minimum of 80 coccospheres per sample with scanning electron microscopy (SEM) using either a TM3000 (Hitachi High-Technologies, Tokyo, Japan) or a Quanta 250 (FEI, Hillsboro, Oregon, USA). Classification followed Young et al. (2003). To estimate the absolute abundances of each species within the Noelaerhabdaceae family, which are difficult to distinguish using light microscopy, the relative abundance of each Noelaerhabdaceae species determined with SEM counts was multiplied by the absolute abundance of total Noelaerhabdaceae cells determined from light microscopy counts. SEM images were also used to measure the minimum and maximum coccosphere diameters and coccolith lengths of each Noelaerhabdaceae species (ImageJ software version 1.48 for Mac OS X). Also, *E. huxleyi* cells were categorized according to Young et al. (2003), based on the distal shield and central plate of coccoliths. For analysis, they were grouped further: lightly calcified coccoliths exhibited delicate distal shield elements that were well separated from each other extending from the central area to the outer rim. The central element was completely open, and central area elements were either lacking, lath like, or plate like (Fig. 2). These corresponded to the morphotypes B, B/C, C, and O (Young et al., 2003; Hagino et al., 2011), a grouping that is supported by recent genetic evidence (Krueger-Hadfield et al., 2014). Moderately calcified coccoliths, corresponding to morphotype A (Young et al., 2003; Hagino et al., 2011), showed thicker distal shield elements that were fused near the central area and often at the rim but were otherwise separated and a grill central area within a cleanly delimited tube. Two over-calcified morphotypes were observed. One corresponded to the morphotype A over-calcified type reported in the Bay of Biscay (Smith et al., 2012) with coccolith central areas completely covered or nearly completely

covered by elements of the central tube, but distal shield elements not fused (here referred to as A_CC). The second, which we refer to as R/over-calcified, corresponded to the R morphotype (distal shield elements fused and slits closed), which exhibited a continuous variation from a wide and open central area (Young et al., 2003) to the extreme forms, so far reported only in the eastern South Pacific (Beaufort et al., 2011), where tube elements had completely or partially overgrown the central area.

2.4 Isolation of *E. huxleyi* strains

Clonal isolates of coccolithophores were obtained from some stations through isolation of calcified cells using an Influx Mariner cell sorter as described previously (Von Dassow et al., 2012; Bendif et al., 2016). During the NBP cruise, the Influx Mariner was in a portable onboard laboratory and isolation of coccolithophores occurred within 6 h of sample collection. For other samplings, live seawater samples were hand-carried to Concepción in a cooler with chilled water, and calcified cells were isolated within 24 h (without exposure to light or nutrient addition to minimize possible clonal reproduction between sampling and cell isolation). Calcified strains were identified using SEM and maintained at 15 °C (Bendif et al., 2016).

2.5 Experimental testing of *E. huxleyi* responses to high CO₂ and low pH

The experiment was performed at the OA test facility of the Calvoco Marine Laboratory of the Universidad Austral de Chile (Torres et al., 2013). The aim was to investigate the effects of short-term exposure to high-CO₂-low-pH conditions similar to those occurring in an upwelling event. The focus was on determining whether there were differences between the heavily calcified morphotypes and moderately calcified morphotypes in response to short-term exposure to CO₂, as would be expected to be experienced by phytoplankton cells from surrounding surface waters inoculating recently upwelled water, where both mooring-mounted and drifter-mounted sensors show pulses of high CO₂ over periods of about a week (Friederich et al., 2008). Experiments were conducted in temperature-controlled water baths at 15 °C, with light intensities of 75 $\mu\text{mol photons m}^{-2} \text{s}^{-1}$ in a 14:10 h light:dark cycle. Culture media were prepared from seawater collected in wintertime from the Quintay coast (central Chile); aged for > 1 month; enriched with 176 μM of nitrate, 7.2 μM of phosphate, and with trace metals and vitamins as described for K/2 medium (Keller et al., 1987); and sterilized by filtration through 0.2 μm Stericups (Merck Millipore, Billerica, MA, USA). Strains were acclimated to light and temperature conditions for at least two consecutive culture transfers, maintaining cell density below 200.000 cells mL⁻¹ and ensuring exponential growth during the acclimation phase. Prior to inoculation, 4.5 L in 8 L

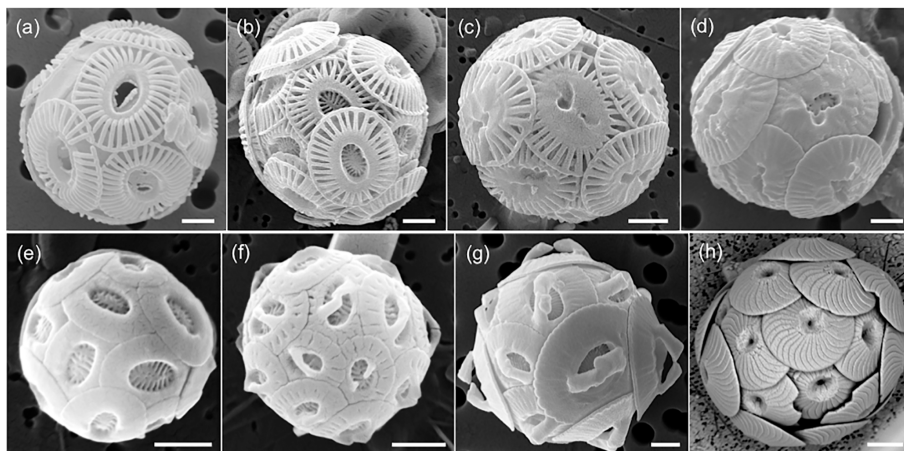


Figure 2. The most abundant coccolithophores in the SE Pacific. (a–d) Morphotypes of *E. huxleyi*: lightly calcified (a), moderately calcified A morphotype (b), morphotype A_CC (c), morphotype R/over-calcified (d). *Gephyrocapsa parvula* (e), *G. ericsonii* (f), *G. muelleriae* (g), and *Calcidiscus leptoporus*. Scale bars are 1 µm (a–g) and 3 µm (h).

cylindrical clear polycarbonate bottles (Nalgene) was continuously purged with humidified air with a $p\text{CO}_2$ of 400 and 1200 µatm for 24–48 h at the experimental temperature to allow the carbonate system to equilibrate (controlled with pH readings) as described in detail in Torres et al. (2013). When pH values had stabilized, four experimental bottles per strain per treatment were inoculated at an initial density of 800 cells mL^{-1} (day 0), and aeration with the air– CO_2 mixes was continued. Daily measures of pH at 25 °C were made potentiometrically at 25.0 °C using a Metrohm 826 pH meter (nominal accuracy ± 0.003 pH units) (Metrohm, Herisau, Switzerland) with an Aquatrode Plus with Pt 1000 (Metrohm 60 253 100) electrode calibrated with tris buffer using established methodology (DOE, 1994; Torres et al., 2013). Samples for TA measurement were taken on day 0 and at the end of the experiment and measured for calculation of full carbonate chemistry parameters as described above for natural seawater samples.

Daily cell counts were performed from day 2 using a Neubauer hemocytometer (as cells were too dilute for this method on day 0). Growth rate was calculated as specific growth rate μ (day^{-1}) = $\ln(N_f/N_0)/\Delta t$, where N_0 and N_f are the initial and final cell concentrations and Δt is the time interval (days). The experimental cultures were harvested before cell concentrations reached 90 000 cells mL^{-1} to minimize changes to the carbonate system from calcification and photosynthesis based on previous studies using R morphotype strains (Rokitta and Rost, 2012). Samples for measurement of POC and PIC were taken by filtering four 250 mL samples on 47 mm GF/F filters (pre-combusted for overnight at 500 °C), which were then dried and stored in aluminium envelopes prior to measurement of C content by the Laboratorio de Biogeoquímica y Isotopos Estables Aplicados at the Pontificia Universidad Católica using a Flash EA2000 elemental analyzer (Thermo Scientific, Waltham, MA, USA),

with a standard error level calculated to be within 0.008 mg C according to linear regression of calibration curves using acetanilide. For each culture, total carbon (TC) was measured on two replicate filters while POC was measured on two replicate filters after treatment by exposure for 4 h to 12 NHCl fumes (Harris et al., 2001; Lorrain et al., 2003). PIC was calculated as the difference between the TC and POC. POC and PIC concentrations were normalized to cell number, and POC and PIC production rates were obtained by multiplying cell-normalized POC and PIC quotas with specific growth rates. Samples were filtered and processed as described above for SEM analysis. For flow cytometry, 1.8 mL samples were fixed by adding 0.2 mL of a solution of 10 % formaldehyde, 0.5 % glutaraldehyde, and 100 mM borate with a pH of 8.5 (which was stored frozen and thawed immediately before use).

SEM and flow cytometric assessments and analyses of coccoliths

Morphological analysis was performed on three replicates of each strain with a scanning electron microscope (Quanta 250) and images were analyzed with ImageJ. Attached coccoliths were measured following Rosas-Navarro et al. (2016). On average, a total of 606 (min. 418) coccoliths per treatment were analyzed. Coccoliths were classified into complete, incomplete, and malformed (Rosas-Navarro et al., 2016). In the R/over-calcified strains, fusion of radial elements and the overgrowth of inner tube elements of the distal shield complicated finer-scale assessments of coccolith formation. Therefore, we were highly conservative in categorizing coccoliths and grouped incomplete and malformed coccoliths for statistical analysis. Of all coccospheres imaged, only coccoliths that were oriented upwards (towards the beam) were selected for measurement so that coccolith

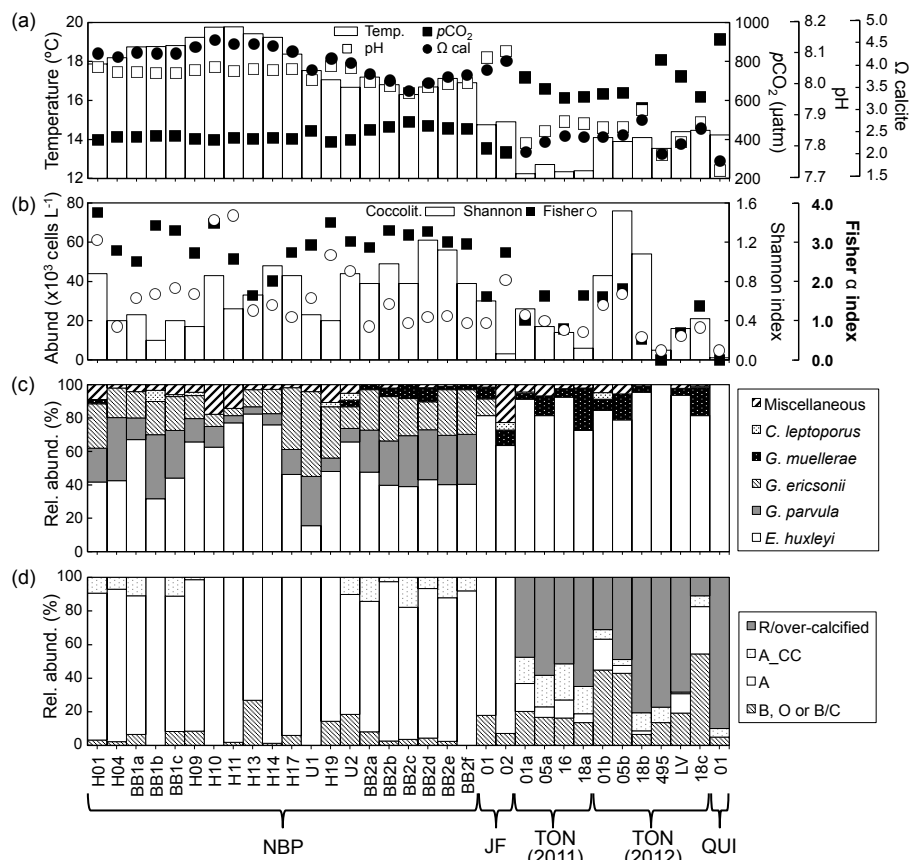


Figure 3. Environmental conditions, coccolithophore community, and *E. huxleyi* morphotypes. (a) Temperature, pH, CO₂, and Ω_{calcite}. (b) Coccolithophore abundance and Shannon and Fisher's alpha diversity indices. (c) Relative abundance of principal coccolithophore taxa. (d) Relative abundance of *E. huxleyi* morphotypes. The lightly calcified morphotypes B, O, and B/C have been grouped together.

length measurements were not affected by viewing angle. This meant that an average of 68 coccoliths were measured per strain per treatment. Measurements included coccolith length, the total area of the central area (defined by the inner end of distal shield radial elements), and the portion of the central area which was not covered by the inner tube.

Flow cytometry was performed using a BD Influx equipped with a 488 nm laser and small particle detector with polarization optics. The laser, optics, and stream were aligned using 3 µm Ultra Rainbow Fluorescent Particles (Spherotech, Lake Forest, IL, USA). The trigger was set on forward scatter light with the same polarization as the laser, with trigger level adjusted for each strain to ensure that all detached coccoliths could be detected. Cells were distinguished by red fluorescence (at 692 nm; due to chlorophyll). Detached coccoliths and calcified cells were distinguished as previously described (Von Dassow et al., 2012). Briefly, calcite-containing particles are above the diagonal formed from optically inactive particles on a plot of forward scatter with polarization orthogonal to the laser vs. forward scatter with polarization parallel to the laser. Also, calcite-

containing particles are high in side scatter. Non-calcified cells fall on the diagonal formed by other particles, including cell debris, bacteria (if present), and calibration or alignment particles. Parameters analyzed included the number of detached coccoliths, percentage of calcified cells, relative change in depolarization of forward scatter light by detached coccoliths, and relative changes in red fluorescence (due to chlorophyll) of cells. All samples for a given treatment and strain were run on the same day with the same settings.

2.6 Statistical analysis

To test for significant correlations of environmental parameters (including carbonate chemistry) on coccolithophore community composition or *E. huxleyi* morphotype composition in the natural samples, redundancy analysis (RDA) was performed (see Supplement). For most analyses, we selected only data from the surface when multiple depths were available (see Sect. S1 in the Supplement for comparison of surface to deeper samples).

Data from experimental results were analyzed in Prism 6 (GraphPad software, Inc., La Jolla, CA, USA) using two-

way ANOVA followed by Sidak post hoc pairwise analysis with correction for multiple comparison. Prior to testing, the PIC / POC ratio was \log_2 -transformed while percentages (e.g., percentage of area, percentage of calcified cells) were expressed as proportions and arcsine-square-root transformed to permit the use of parametric testing. Significance was judged at the $p < 0.05$ level.

3 Results

3.1 Changes in coccolithophore species and *E. huxleyi* morphotypes in natural communities vs. oceanographic conditions

Surface pH (< 10 m depth) at sampling sites ranged from 7.73 (in the El Quisco 2012 sampling) to 8.11 (in the JF sampling). In terms of carbonate chemistry, the surface waters of the ESP showed a general pattern of increasing CO₂ and decreasing pH as one moves from open ocean waters to the Chilean coastal upwelling zones; however, as expected, waters were never corrosive for calcite (Fig. 3a). More generally, the NBP and JF, as well as TON and QUI surveys, were conducted at a relatively low (average $411.2 \pm 41.3 \mu\text{atm}$; $N_{\text{samples}} = 27$) and high (average $696.6 \pm 110 \mu\text{atm}$; $N_{\text{samples}} = 14$) CO₂ levels, respectively.

Coccolithophore numerical abundances ranged from 1×10^3 cells to 76×10^3 cells L⁻¹ (59 total samples) (Fig. 3b). A total of 40 coccolithophore species were found inhabiting the eastern South Pacific during the sampling period (Table S4). The Shannon diversity index ranged from 1.5 down to 0, while the Fisher's alpha index ranged from 4.0 down to 0, and both indices showed coccolithophore diversity was lowest in the most acidified natural waters (Fig. 3a and b).

Five species of the Noelaerhabdaceae family were observed, including *E. huxleyi*, *Gephyrocapsa ericsonii*, *G. muelleriae*, *G. oceanica*, and *G. parvula*, the last of which was recently reassigned from the genus *Reticulofenestra* to the genus *Gephyrocapsa* (Bendif et al., 2016). The Noelaerhabdaceae family numerically dominated all coccolithophore communities observed, representing between 72.2 and 100 % (average 94.1 ± 6.9 %) of all coccolithophores in all samples observed. The most abundant coccolithophore outside this family was *Calcidiscus leptoporus*, present at 36 % of stations and ranging in relative abundance from 0.9 % to 25.4 % (average 5.6 ± 6.9 %). Within Noelaerhabdaceae, *E. huxleyi* was found in every sample and exhibited relative abundances ranging from 15.5 to 100 % of total coccolithophores (Fig. 3c). While *E. huxleyi* represented up to 100 % of the coccolithophore community in high-CO₂ waters on the central Chilean coast (stations in groups “TON (2011)”, “TON (2012)”, and “QUI”), it was observed in lower relative abundances of samples taken both further offshore (NBP samples H01–U2 and JF stations) and to the north (NBP samples BB2a–BB2f), where indices of coccolithophore diver-

sity were generally higher (Fig. 3b and c). *Gephyrocapsa ericsonii* and *G. parvula* were essentially excluded from high-CO₂ waters.

R/over-calcified morphotypes dominated *E. huxleyi* populations in high-CO₂ waters near the central Chilean coast (samples in groups “TON (2011)”, “TON (2012)”, and “QUI” in Fig. 3; see also Fig. S3), representing on average 57.2 ± 22.9 % (range 11 to 90 %) (Fig. 3d). In contrast, moderately calcified A morphotype coccospheres dominated *E. huxleyi* populations in all low-CO₂ waters both further offshore (NBP samples H01–U2 and JF stations) and near the coast to the north (NBP stations BB2a–BB2f) (Figs. 3d and S3). The other over-calcified morphotype A_CC, a form characteristic of the Subtropical Front in the western Pacific (Cubillos et al., 2007), represented less than 20 % of total coccolithophores and did not follow a clear pattern. The lightly calcified morphotypes were usually rare except in some of the samples from near the Tongoy–Punta Lengua de Vaca upwelling (Stations in groups “TON (2011)” and “TON (2012)” in Fig. 3d), where they seemed to be associated with intermediate CO₂ levels.

3.2 Phenotypes of *E. huxleyi* clonal isolates compared to natural populations from the high-CO₂ and low-CO₂ waters

Throughout the field campaigns, a total of 260 Noelaerhabdaceae isolates were obtained and analyzed morphologically (Table 1; note that strains from stations nearby in time and space have been grouped). There was a bias towards isolating the dominant type within both the Noelaerhabdaceae and *E. huxleyi* species complex at each station, and only 2 % of the maintained isolates were from the *Gephyrocapsa* genus, suggesting that these closely related species are not as readily cultured as *E. huxleyi*. The lightly calcified morphotype also remained poorly represented in culture compared to the natural communities, and the A_CC type appeared moderately overrepresented. However, among the R/over-calcified and moderately calcified A morphotypes, the dominant morphotype obtained in culture always reflected the dominant morphotype in the natural community. Three representative R/over-calcified morphotype strains, showing different degrees of overlap of the central area, and two representative A morphotype strains from offshore waters were chosen for experimental analysis (Fig. 4).

3.3 Responses of different *E. huxleyi* morphotypes to high CO₂ and low pH

Aeration with CO₂–air mixes prior to inoculation successfully equilibrated $p\text{CO}_2$ levels, which remained close to target levels throughout the experiment, with final pH values averaging 8.013 ± 0.029 under the control condition (400 μatm $p\text{CO}_2$) and 7.574 ± 0.021 under high-CO₂–low-pH conditions (1200 μatm $p\text{CO}_2$) (Table 2). Seawater remained super-

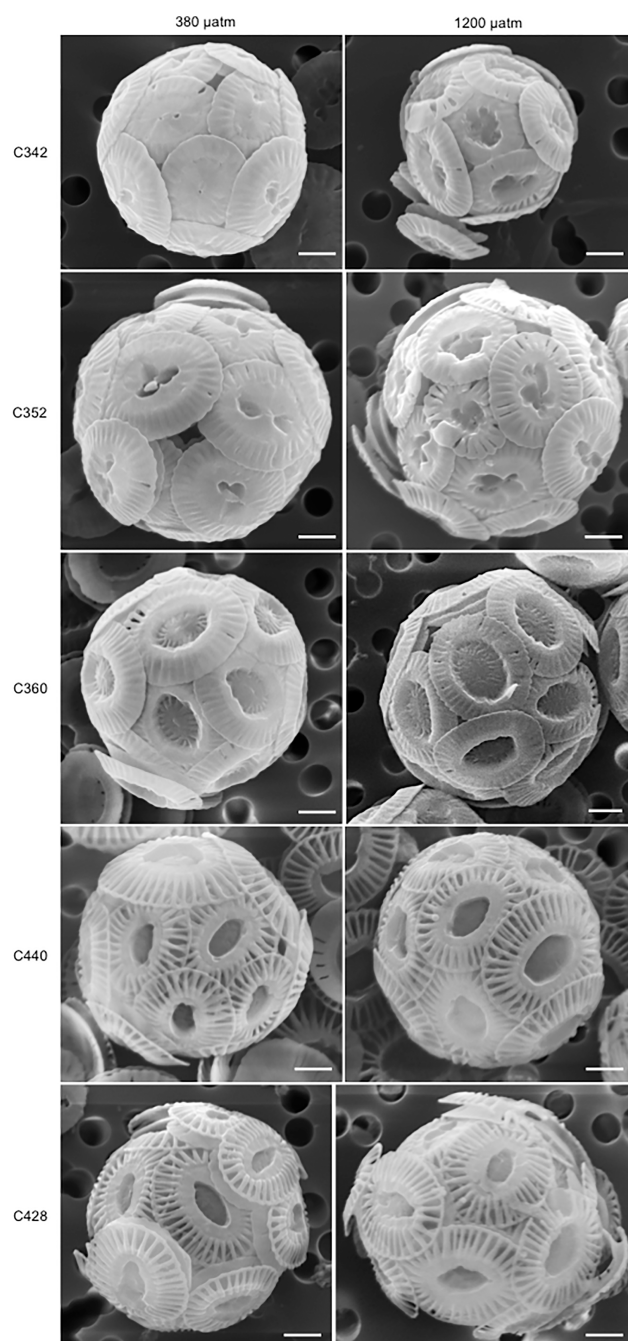


Figure 4. Representative coccospheres from each strain and treatment tested in the experiment. CHC342 was isolated from the Pacific coast of Isla de Chiloé (41.9° S, 74.0° W) in November 2012. CHC352 and CHC360 were isolated from the Punta Lengua de Vaca upwelling center (30.3° S, 71.7° W) in November 2012. CHC440 and CHC428 were isolated from the station farthest west in the Pacific (station H10, at 16.7° S, 86° W) during the NBP1305 cruise in July 2013.

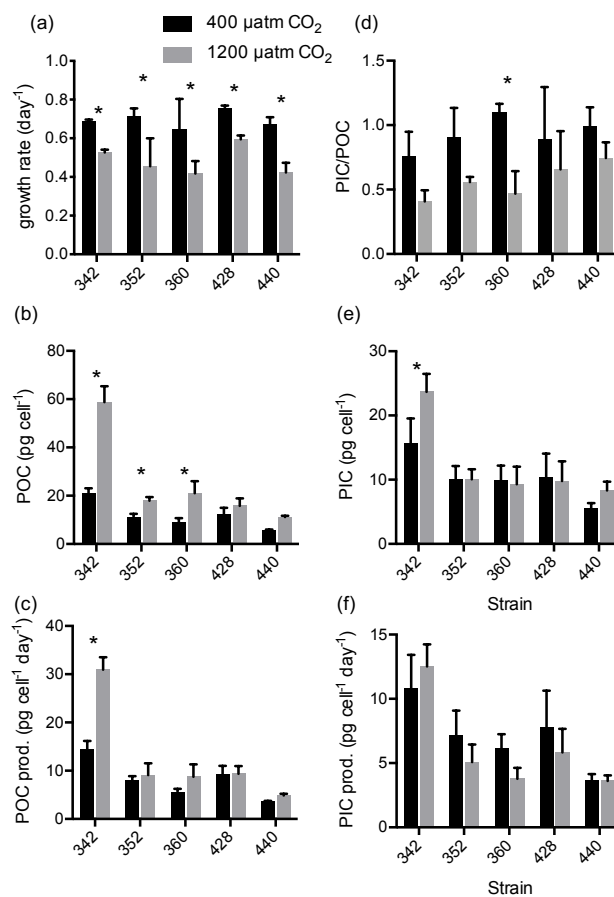


Figure 5. Growth rates (a), POC quotas (b), POC production rates (c), PIC / POC (d), PIC quotas (e), and PIC production rates (f) of *E. huxleyi* strains in response to 400 μatm (black bars) and 1200 μatm (grey bars) CO₂ treatments. See Table 3 for global two-way ANOVA results. The * indicates a significant difference ($p < 0.05$) in pairwise comparison between the two CO₂ treatments for a given strain, as judged by Sidak post hoc testing with correction for multiple comparison.

saturated with respect to calcite ($\Omega_{\text{calcite}} > 1$) and Ω_{calcite} values achieved were in a similar range to those seen in the natural waters sampled (Fig. 2), with final values averaging $\Omega_{\text{calcite}} = 3.252 \pm 0.260$ across strains under the control condition and $\Omega_{\text{calcite}} = 1.423 \pm 0.077$ for the high-CO₂-low-pH condition (Tables 2 and S1). Continued aeration and keeping cell concentration below 90 000 cells mL⁻¹ was mostly successful in minimizing changes in carbonate system parameters. Averaging the mean values for each strain, alkalinity changed by $-187 \pm 132 \mu\text{mol kg}^{-1}$ ($-8.24 \pm 5.86\%$) in the control condition and $-29 \pm 19 \mu\text{mol kg}^{-1}$ ($-1.26 \pm 0.82\%$) under the high-CO₂-low-pH condition. However, for strain CHC342 the change in alkalinity under the control condition was larger ($-18.64 \pm 1.43\%$) (discussed below). This led to a lower final dissolved CO₂ (to $12.4 \pm 0.2 \mu\text{mol kg}^{-1}$) compared to the other four strains ($15.0 \pm 1.3 \mu\text{mol kg}^{-1}$).

Table 1. Noelaerhabdaceae strains isolated during this study. All sites near Tongoy were grouped in 2011 and in 2012, as were the sites at JF in 2011.

Site	Total strains	<i>E. huxleyi</i>				Other species		
		R/over	A_CC	A	Light	<i>G. muel.</i>	<i>G. eric.</i>	<i>G. parv.</i>
TON 2011	132	85 %	10 %	2 %	1 %	2 %	0 %	0 %
JF 2011	34	32 %	35 %	32 %	0 %	0 %	0 %	0 %
TON 2012 ^a	20	90 %	10 %	0 %	0 %	0 %	0 %	0 %
Puñi. 2012 ^b	10	40 %	20 %	40 %	0 %	0 %	0 %	0 %
NBP H1	15	0 %	33 %	67 %	0 %	0 %	0 %	0 %
NBP H10 ^c	28	0 %	21 %	55 %	24 %	0 %	0 %	0 %
NBP BB2	21	0 %	33 %	43 %	0 %	0 %	5 %	19 %

^a Site represented by strains CHC352 and CHC360. ^b Site represented by strain CHC342. ^c Site represented by strains CHC428 and CHC440.

Table 2. Carbonate system parameters during experiment. Means \pm SDs of experimental replicates at the time of inoculation (T_{inoc}) and harvesting (T_{final}) are given. The pH at the experimental temperature is calculated from measured pH at 25 °C. Treatment is specified by CO₂ partial pressure (μatm) of air : CO₂ mix. $p\text{CO}_2$ units are μatm ; alkalinity and [CO₂] units are $\mu\text{mol kg}^{-1}$. The average \pm SDs across strains for cell-free control bottles and mean experimental bottle values are also provided. The last two rows give the average and maximum SDs among replicates among all strains.

Strain	Treat.	$p\text{CO}_2$		Alkalinity		pH		Ω_{calcite}		Dissolved [CO ₂]	
		T_{inoc}	T_{final}	T_{inoc}	T_{final}	T_{inoc}	T_{final}	T_{inoc}	T_{final}	T_{inoc}	T_{final}
342	400	422.0 \pm 38	332 \pm 4	2260 \pm 7	1839 \pm 25	8.020 \pm 0.033	8.029 \pm 0.033	3.531 \pm 0.225	2.891 \pm 0.097	15.8 \pm 1.4	12.4 \pm 0.2
	1200	1314 \pm 27	1257 \pm 36	2264 \pm 5	2207 \pm 19	7.574 \pm 0.008	7.582 \pm 0.008	1.402 \pm 0.026	1.400 \pm 0.022	50.8 \pm 49.4	49.4 \pm 1.0
352	400	402.5 \pm 6	370.0*	2292 \pm 13	2168*	8.042 \pm 0.005	8.035 \pm 0.005	3.591 \pm 0.041	3.494*	15.6 \pm 0.2	14.2*
	1200	1226 \pm 27.6	1341 \pm 65	2274 \pm 12	2161 \pm 20	7.601 \pm 0.007	7.561 \pm 0.018	1.440 \pm 0.015	1.339 \pm 0.057	47.6 \pm 1.1	51.4 \pm 2.5
360	400	441.4 \pm 18.7	457.4 \pm 47.7	2270 \pm 6	2126 \pm 7	8.005 \pm 0.016	7.965 \pm 0.040	3.552 \pm 0.105	3.079 \pm 0.270	16.0 \pm 0.7	16.6 \pm 1.8
	1200	1186 \pm 94.7	1409 \pm 156	2289 \pm 10	2254 \pm 4	7.623 \pm 0.032	7.545 \pm 0.043	1.648 \pm 0.107	1.370 \pm 0.128	43.0 \pm 3.4	51.5 \pm 5.8
428	400	440.3 \pm 21.5	418.5 \pm 12.9	2261 \pm 6	2157 \pm 19	8.004 \pm 0.018	8.004 \pm 0.010	3.537 \pm 0.117	3.328 \pm 0.035	15.9 \pm 0.8	15.3 \pm 0.5
	1200	1259 \pm 6.4	1247 \pm 30.6	2262 \pm 4	2250 \pm 5	7.592 \pm 0.002	7.592 \pm 0.009	1.521 \pm 0.007	1.494 \pm 0.027	45.8 \pm 0.2	45.9 \pm 1.1
440	400	457.4 \pm 26.0	381.6 \pm 5.6	2254 \pm 6	2114 \pm 17	7.988 \pm 0.021	8.033 \pm 0.005	3.259 \pm 0.127	3.469 \pm 0.104	17.3 \pm 1.0	13.8 \pm 0.3
	1200	1487 \pm 32.2	1249 \pm 55.0	2261 \pm 5	2235 \pm 7	7.522 \pm 0.009	7.591 \pm 0.019	1.243 \pm 0.022	1.512 \pm 0.050	56.2 \pm 1.2	45.1 \pm 1.8
Ave. w/o cells	400	434.0 \pm 37.1	396.7 \pm 20.7	2265 \pm 13	2273 \pm 19	8.011 \pm 0.032	8.051 \pm 0.022	3.482 \pm 0.236	3.698 \pm 0.124	16.2 \pm 1.5	14.9 \pm 0.6
	1200	1286 \pm 584.2	1290 \pm 28.1	2268 \pm 8	2239 \pm 58	7.585 \pm 0.036	7.583 \pm 0.011	1.444 \pm 0.135	1.461 \pm 0.038	49.1 \pm 4.9	47.7 \pm 0.9
Ave. with cells	400	432.7 \pm 21.0	392.0 \pm 47.8	2267 \pm 15	2081 \pm 137	8.012 \pm 0.020	8.013 \pm 0.029	3.494 \pm 0.133	3.252 \pm 0.260	16.1 \pm 0.7	14.5 \pm 1.6
	1200	1294 \pm 117.1	1301 \pm 72.1	2270 \pm 12	2241 \pm 22	7.582 \pm 0.038	7.574 \pm 0.021	1.451 \pm 0.149	1.423 \pm 0.077	48.4 \pm 5.0	48.1 \pm 3.1
Ave. SD	400	22.1	17.6	8	17	0.018	0.016	0.123	0.127	0.8	0.7
	1200	37.5	68.6	7	11	0.012	0.020	0.035	0.057	1.4	1.8
Max. SD	400	38.2	47.7	13	25	0.033	0.040	0.225	0.270	1.4	2.5
	1200	94.7	156	12	20	0.033	0.043	0.107	0.128	3.4	5.8

* Only one alkalinity sample was analyzed from the 400 $p\text{CO}_2$ treatment for strain CHC352, as three were lost in transit between labs.

High CO₂ and low pH significantly reduced the growth rate in all strains and there was no significant interaction between strain and high-CO₂-low-pH effects on growth rate (Fig. 5a; see Table 3 for global two-way ANOVA statistics). High CO₂ and low pH increased POC quota (POC cell⁻¹) in all strains. However, the interaction between strain and high CO₂ and low pH was significant (Fig. 5b; Table 3). The increase in POC quota was not significant in moderately calcified strains CHC428 and CHC440, while the hyper-calcified strain CHC342 exhibited the highest POC quota and the highest increase under OA conditions. The effect of high CO₂ and low pH on the POC production rate varied among strains: high CO₂ and low pH increased POC production in most strains, except for the moderately calcified strain CHC428 (Fig. 5c; Table 3). However, the change in POC production was significant in post hoc pairwise com-

parisons only for CHC342, in which it increased by 116 % ($p < 0.0001$). Except for strain CHC342, which exhibited the most over-calcified coccoliths (completely fused distal shield radial elements and central area nearly completely overgrown by tube elements), when all strains were considered, neither POC quota nor POC production were consistently different in R/over-calcified vs. A morphotype strains.

PIC / POC ratios dropped under high CO₂ and low pH in all strains (Fig. 5d). It is notable that the smallest changes in PIC / POC occurred in the two strains of moderately calcified morphotypes originating from offshore, low- $p\text{CO}_2$ waters, not the strains with hyper-calcified or heavily calcified morphotypes originating from coastal waters naturally exposed to high CO₂ and low pH. However, although the effect of high-CO₂-low-pH conditions was globally significant across all strains according to a two-way ANOVA (Table 3), in pair-

Table 3. Global two-way ANOVA results for growth and biogeochemical parameters of strains exposed to high-CO₂–low-pH conditions vs. control CO₂ treatment. PIC / POC values were log₂-transformed prior to testing.

		Growth rate	POC	POC prod	PIC	PIC prod.	PIC / POC
Source of variat.	Interact.	2.63 %	21.7 %	18.8 %	10.3 %	6.00 %	8.15 %
	Strain	13.7 %	62.8 %	77.5 %	71.3 %	69.2 %	10.9 %
	CO ₂	60.9 %	23.0 %	9.67 %	3.68 %	2.13 %	37.8 %
<i>F</i> values	Interact.	$F_{4,29} = 0.926$	$F_{4,25} = 36.1$	$F_{4,25} = 27.0$	$F_{4,25} = 3.08$	$F_{4,25} = 1.65$	$F_{4,25} = 1.15$
	Strain	$F_{4,29} = 4.83$	$F_{4,25} = 105$	$F_{4,25} = 111.0$	$F_{4,25} = 21.3$	$F_{4,25} = 19.0$	$F_{4,25} = 1.54$
	CO ₂	$F_{1,29} = 85.7$	$F_{1,25} = 153$	$F_{1,25} = 55.6$	$F_{1,25} = 4.38$	$F_{1,25} = 2.33$	$F_{1,25} = 21.3$
<i>p</i> values	Interact.	0.463	< 0.0001	< 0.0001	0.0343	0.194	0.358
	Strain	0.0041	< 0.0001	< 0.0001	< 0.0001	< 0.0001	0.222
	CO ₂	< 0.0001	< 0.0001	< 0.0001	0.0466	0.139	0.0001

Table 4. Global two-way ANOVA results for coccosphere and coccolith parameters of strains exposed to high-CO₂–low-pH conditions vs. control CO₂ treatment. Proportions of central area covered and of incomplete or malformed coccoliths were arcsine-square-root transformed prior to testing.

		Coccosphere diameter	Coccolith length	Proportion central area covered	Proportion of coccoliths incompl. or malform.
Source of variat.	Interact.	7.58 %	34.7 %	12.3 %	4.40 %
	Strain	53.7 %	25.3 %	53.3 %	18.0 %
	CO ₂	4.76 %	0.396 %	29.2 %	55.4 %
<i>F</i> values	Interact.	$F_{4,19} = 1.071$	$F_{4,19} = 4.62$	$F_{4,19} = 21.9$	$F_{4,19} = 1.18$
	Strain	$F_{4,19} = 7.595$	$F_{4,19} = 3.37$	$F_{4,19} = 94.7$	$F_{4,19} = 4.83$
	CO ₂	$F_{1,19} = 2.689$	$F_{1,19} = 0.211$	$F_{1,19} = 207$	$F_{1,19} = 59.6$
<i>p</i> values	Interact.	0.398	0.0090	< 0.0001	0.351
	Strain	0.0008	0.0304	< 0.0001	0.0074
	CO ₂	0.118	0.652	< 0.0001	< 0.0001

wise post hoc comparisons the drop in PIC / POC ratio was only significant in CHC360 ($p = 0.005$). Also, the effect of strain on PIC / POC was not significant and there was no significant interaction between strain and high CO₂ and low pH (Table 3). PIC quotas varied among strains and the effect of high CO₂ and low pH also differed among strains (Fig. 5e; Table 3). The highest PIC quota was recorded in the hyper-calcified strain CHC342 and the lowest in the moderately calcified strain CHC440. High CO₂ and low pH increased PIC quota significantly in strain CHC342 (pairwise post hoc test, $p = 0.0039$), but did not change PIC quota or the change was not significant in other strains. PIC production varied among strains (Fig. 5f; Table 3) but there were no significant effects of high CO₂ and low pH or interaction between strain and high CO₂ and low pH (Table 3).

Decreases in alkalinity correlated with PIC (Table 2, Fig. S4). However, for strains CHC342 and CHC440 the drop in alkalinity was more than 2-fold greater than what would have been predicted from PIC under control conditions (but not under the high-CO₂–low-pH condition) (Supplement Sect. S3, Fig. S4). When data from strains CHC342 and CHC440 were excluded, the linear relationship between

measured and predicted change in alkalinity was not significantly different than 1 : 1 (Fig. S4).

R/over-calcified coccoliths were not more resistant to high CO₂ and low pH than A morphotype coccoliths. High CO₂ and low pH significantly affected at least one morphological parameter measured in all but the A morphotype strain CHC440 (Figs. 4 and 6). The coccosphere diameters did not change significantly under high CO₂ and low pH in any of the strains (Fig. 6d; Table 4). Coccolith lengths showed inconsistent and mostly insignificant changes among strains. In the global two-way ANOVA comparison, there was an interaction between treatment and strain (Table 4), but the only significant change under high CO₂ and low pH detected with post hoc pairwise comparisons among treatments was a small decrease in CHC428 under high CO₂ and low pH (Fig. 6e; $p = 0.0334$). The percentage of the central area that was uncovered by inner tube elements increased under OA (Fig. 6f). The significant interaction between strain and treatment (Table 4) indicated that the effect of high CO₂ and low pH on this parameter varied among strains. It was most pronounced in strains CHC342 and CHC352, where the inner tube elements were heavily overgrown under low p CO₂, whereas the effect

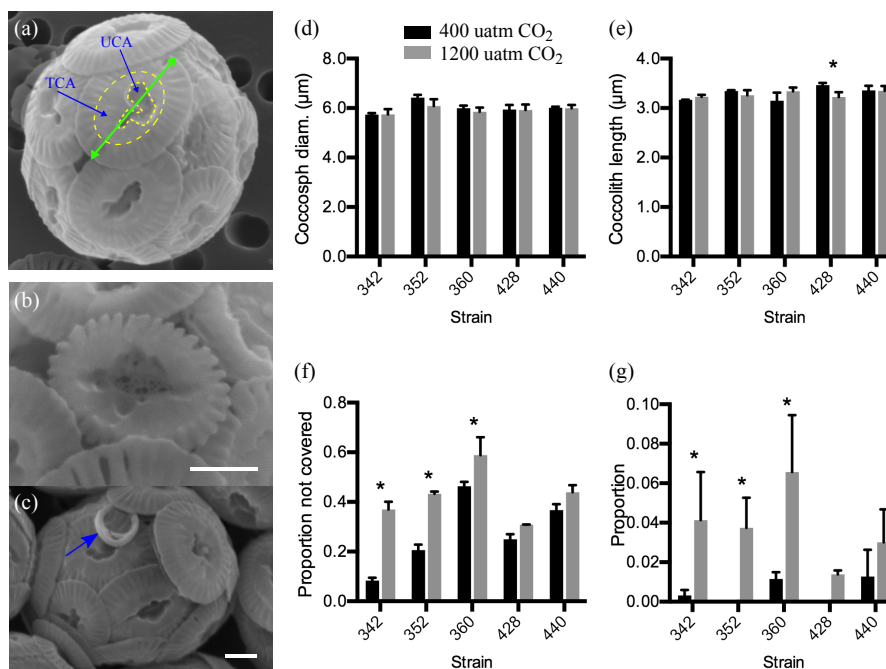


Figure 6. Effects of high- CO_2 -low-pH conditions on coccolithophore morphology. (a) Example illustrating coccolith measurements taken including coccolith length (solid line with two arrow heads), total central area including the inner tube (TCA) (defined by inner terminal of radial elements), and the part of the central area that is uncovered by tube elements (UCA). (b) Example of a coccolith classified as incomplete or malformed. (c) Example of a very incomplete coccolith (arrow). (d) Coccosphere diameters. (e) Coccolith length. (f) Proportion of central area not covered. (g) Proportion of coccoliths that were malformed or incomplete. See Table 4 for global two-way ANOVA results. The * indicates significant difference ($p < 0.05$) in pairwise comparison between the two CO_2 treatments for a given strain, as judged by Sidak post hoc testing with correction for multiple comparison.

was modest in the moderately calcified strains CHC428 and CHC440 (and not significant in pairwise post hoc tests of the effect of treatment within these strains; $p > 0.05$), where the central area was mostly exposed under both conditions. The incidence of incomplete or malformed coccoliths remained very low in all strains and treatments, but high CO_2 and low pH caused a modest but significant increase (Fig. 6g; Table 4), ranging from between 0 and 1.3 % of coccoliths under low CO_2 to between 1.4 and 6.6 % under high CO_2 and low pH. This effect was greatest in R/over-calcified morphotype strains CHC342, CHC352, and CHC360, but there was no significant interaction between strain and treatment in the two-way ANOVA when all strains were considered (Table 4).

Flow cytometric analysis (see example cytogram in Fig. S5) showed significant changes in several cytometric parameters in response to high CO_2 and low pH, which in some cases varied among strains (Fig. 7; Table 5). Relative chlorophyll fluorescence was increased significantly in strains CHC360, CHC440, and CHC428, but dropped significantly in CHC352 (Fig. 7a, Table 5). The proportion of cells which were calcified was high (> 97 %) in all strains under the 400 $\mu\text{atm CO}_2$ control treatment but dropped modestly (0.04 to 7.2 %) in all strains in the OA treatment (Fig. 7b). A significant interaction was detected between strain and

treatment in the proportion of cells calcified (Table 5), and this drop in response to high CO_2 and low pH was greatest in strains CHC360 (average change of -7.2%) and CHC440 (average change of -5.4%), which were the only two strains for which the difference between treatments was judged significant in pairwise post hoc testing. In the control CO_2 treatment, the relative abundance of detached coccoliths, relative to the number of cells, was low (11.9 to 14.4 cell^{-1}) in most strains but high ($63 \pm 34 \text{ cell}^{-1}$) in strain CHC440. Despite significant variability among strains in the relative abundance of detached coccoliths, there were no significant changes under high CO_2 and low pH (Fig. 7c; Table 5). The relative forward scatter depolarization (a proxy for the amount of calcite on a cell (see Von Dassow et al., 2012)) was decreased significantly under high CO_2 and low pH (Fig. 7d; Table 5), an effect which varied among strains (Table 5) and was strongest in strain CHC352. The relative scatter depolarization of detached coccoliths was also decreased under high CO_2 and low pH (Fig. 7e; Table 5), an effect that varied among strains and was largest in CHC352 and CHC428.

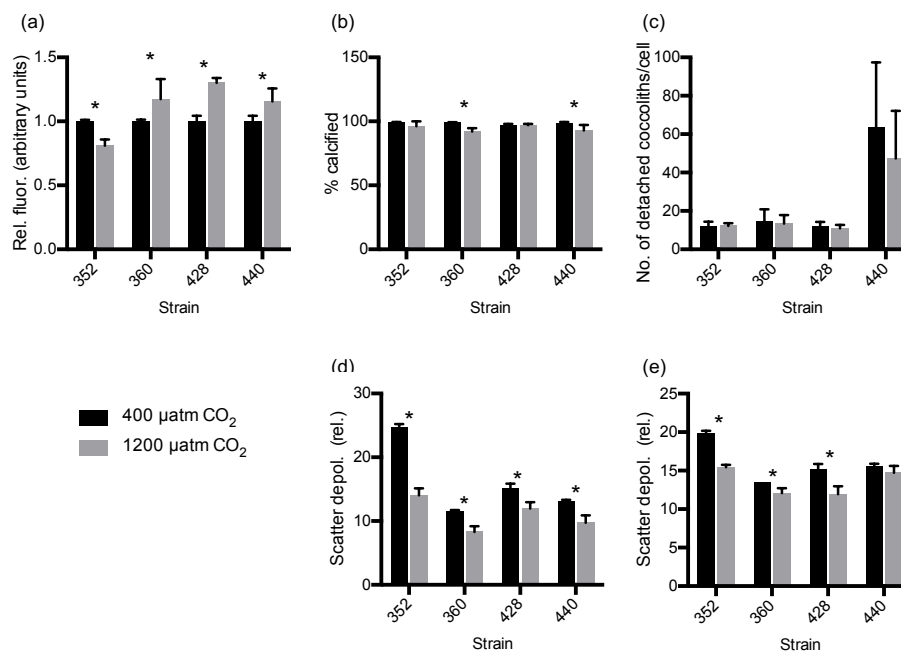


Figure 7. Effects of high- CO_2 treatment on flow cytometric properties of cells and detached coccoliths for all treatments and strains. Strain CHC342 is not shown because samples were lost in transit between labs. Shown are the relative fluorescence (compared to control treatment) (a), the proportion of cells that were calcified (b), abundance of detached coccoliths divided by cell abundance (c), relative FSC (scatter depolarization) of cells (d), and detached coccoliths (e). Fluorescence and FSC units are relative and the voltage for the detector for FSC perpendicularly polarized was 2-fold higher, resulting in a sensitivity approximately 2 orders of magnitude higher. Scatter depolarization was calculated for every particle as the ratio of FSC with polarizations perpendicular vs. parallel to the laser, normalized by the same ratio for non-optically active particles within the same sample. The * indicates significant difference ($p < 0.05$) in pairwise comparison between the two CO_2 treatments for a given strain, as judged by Sidak post hoc testing with correction for multiple comparison.

Table 5. Global two-way ANOVA results for flow cytometric parameters. The percentages of calcified cells were expressed as a fraction and arcsine-square-root transformed prior to testing.

		Rel. red fluoresce.	% calcified	No. detached coccol.	Rel. scatter depol. cells	Rel. scatter depol. detached liths
Source of variat.	Interact.	35.0 %	18.9 %	2.27 %	11.2 %	7.85 %
	Strain	34.7 %	6.42 %	67.8 %	55.8 %	57.9 %
	CO_2	13.5 %	38.7 %	1.09 %	25.4 %	22.8 %
F values	Interact.	$F_{3,20} = 16.0$	$F_{3,20} = 3.62$	$F_{3,20} = 0.525$	$F_{3,20} = 36.5$	$F_{3,20} = 12.3$
	Strain	$F_{3,20} = 15.9$	$F_{3,20} = 1.23$	$F_{3,20} = 15.7$	$F_{3,20} = 182$	$F_{3,20} = 90.6$
	CO_2	$F_{1,20} = 18.5$	$F_{1,20} = 22.2$	$F_{1,20} = 0.757$	$F_{1,20} = 249$	$F_{1,20} = 107$
p values	Interact.	< 0.0001	0.0309	0.670	< 0.0001	< 0.0001
	Strain	< 0.0001	0.326	< 0.0001	< 0.0001	< 0.0001
	CO_2	0.0003	0.0001	0.395	< 0.0001	< 0.0001

4 Discussion

While an increasing number of studies have focused on examining the potential for adaptation to OA through long-term laboratory experiments, this study has taken an alternative approach, to test for local adaptation to short-term high- CO_2 and low-pH exposure in populations of cosmopolitan phytoplankton found in waters that experience naturally acidi-

fied conditions due to upwelling of high- CO_2 water. A similar approach has recently been taken in a variety of invertebrate species (Padilla-Gamiño et al., 2016; Gaitán-Espitia et al., 2017; Vargas et al., 2017), finding both benthic and meroplanktonic animals, coralline algae, and holoplanktonic copepods do exhibit local adaptation in regions experiencing naturally high fluctuations in pH and CO_2 .

This study confirms that R/over-calcified forms of *E. huxleyi* which appear exceptionally robust (as both the central area is extensively overgrown and the distal shield elements are fused) occur in the coastal zone of central to northern Chile. This was previously hinted from two sampling points and times (Beaufort et al., 2011) and has now been documented in separate years. Within the subtropical and tropical eastern South Pacific, the presence of these morphotypes coincides both with high CO₂ and low pH (low Ω_{calcite}) as well as with lower temperature (Fig. S3), and it is difficult to separate these two parameters. However, at the lowest end of the *E. huxleyi* temperature range, populations are often found to be dominated by more lightly calcified morphotypes (Cubillos et al., 2007); thus a relationship to temperature would have to be very nonlinear. More importantly, while a “type A over-calcified” type was reported in winter waters of the Bay of Biscay (Smith et al., 2012) and a heavily calcified type “A*” was reported in the Benguela coastal upwelling (Henderiks et al., 2012) (both exhibiting only overgrowth of the central area by tube elements but not fusion of distal shield elements), the exceptionally robust R/over-calcified forms seen near Chile have not been reported from these other upwelling systems. Therefore, we set out here to test the simplest hypothesis – focusing on a single factor – that these forms may be adapted to resist high-CO₂–low-pH conditions.

The use of targeted flow cytometry and cell sorting was successful in obtaining representatives of the different forms of *E. huxleyi* in monoculture to test whether the correlation between phenotype and environment indeed reflected local adaptation. Two of the R/over-calcified strains chosen for experimental tests (CHC352 and CHC360) originated from the high-CO₂ upwelling near Tongoy–Punta Lengua de Vaca (Table 1). Strain CHC342 originated from Puñihuil along the outer (western) coast of Isla de Chiloé (41.9° S). Although we lack carbonate system data from this site, the Isla de Chiloé is located approximately where the West Wind Drift arrives at the continent and turns north to form the Humboldt Current System (Thiel et al., 2007). Thus we considered that CHC342, exhibiting a highly over-calcified R morphotype, might represent the southern end of the *E. huxleyi* populations that drift north and experience high-CO₂–low-pH upwelling conditions. We compared these three R/over-calcified strains to two A morphotype strains isolated from low-CO₂ waters at a site 1000 km from the nearest shore (NBP cruise station H10 in Figs. 1 and 3). Organisms in such waters are expected to experience very low fluctuations in pH (Hofmann et al., 2011), and so these strains were expected to exhibit low resistance to transient high-CO₂–low-pH conditions.

The high-CO₂–low-pH condition (1200 $\mu\text{atm CO}_2$) tested was chosen to represent recently upwelled water based on Torres et al. (1999) compared to CO₂ levels in non-upwelling surface waters (400 μatm). The high CO₂ level of 1200 μatm was also chosen considering previous laboratory studies of

the response of *E. huxleyi*: results of acclimated growth rate in response to short-term changes in the carbonate system manipulated by bubbling have been reported in several studies for two R morphotype strains isolated from the Tasman Sea (where high-CO₂ upwelling is not known), of which four studies reported no significant effect on growth rate of intermediate CO₂ levels (Langer et al., 2009; Shi et al., 2009; Richier et al., 2011; Rokitta and Rost, 2012) compared to one which reported a decrease at 750 μatm (Iglesias-Rodriguez et al., 2008). For other *E. huxleyi* strains, results at intermediate CO₂ levels are not consistent among either studies or even among strains used in the same study, while all strains tested at higher levels ($\geq 950 \mu\text{atm}$) have shown slight to pronounced decreases in growth rate (Langer et al., 2009).

The bloom-former *E. huxleyi* is often considered a fast-growing pioneer phytoplankton species (Paasche, 2002). However, calcification is costly and most evidence suggests it may confer protective or defensive functions (Monteiro et al., 2016). Thus we considered both growth rate and calcification–morphological responses when analyzing potential adaptation. Surprisingly, we found no evidence that the exceptionally robust form was more resistant to high CO₂ than moderately calcified forms that seemed to be excluded from the high-CO₂ upwelling waters.

The high-CO₂–low-pH treatment reduced growth rate in all strains. The decrease in growth rate was accompanied by an increase in POC quota. This might suggest that cells were getting bigger, compensating for a decreased rate of cell division (as the increase in POC production rate was not significant in four of the five strains tested). However, the decrease in growth rate was also reflected in a decrease in culture in vivo fluorescence (data not shown). Changes in coccosphere diameter were insignificant, and changes in cellular fluorescence measured by flow cytometry were small and consistent with only a small possible increase in cell biomass (and not in all strains, as CHC352 showed a decrease in this parameter). Among the few previous studies in which a period of pre-acclimation to CO₂ was not used prior to growth measurements, inconsistent and non-significant effects of growth have been seen in two R morphotype strains NZEH (PLY M219) (Shi et al., 2009) and RCC1216 (Richier et al., 2011). Another study comparing several morphotypes isolated from the Southern Ocean reported that two “A/over-calcified” strains (similar to the R morphotype strain CHC360, but with distal shield radial elements not consistently fused) were relatively resistant to high-CO₂–low-pH treatments compared to both the A morphotype and the lighter B/C morphotype in which growth and calcification were strongly inhibited (Müller et al., 2015a). Thus the R/over-calcified strains tested here, originating from high-CO₂ environments, were surprisingly not resistant to high CO₂. While caution is warranted in comparing the absolute resistance of the R and R/over-calcified morphotypes tested in this study to those tested in the study by Müller et al. (2015a) even when similar high-CO₂–low-pH treatments were tested, the robust conclusion

is that the A morphotypes tested here from the eastern South Pacific were not more sensitive than the R/over-calcified strains from neighboring high-CO₂-low-pH waters.

In strain CHC342, the POC quota exceeded values previously reported in the literature for the species in response to high CO₂ and low pH by more than 3-fold. This occurred in all four replicates, sampled at the same time as the low-CO₂ replicates, so we have no evidence for this increase being a technical artefact. The increase in dissolved CO₂ in the high-CO₂-low-pH condition compared to the control condition was highest in strain CHC342 due to a higher consumption of alkalinity and/or DIC. The levels of dissolved CO₂ in the control (400 µatm pCO₂) condition for all strains fell in a range (12.4–16.6 µmol kg⁻¹) that should be saturating for photosynthesis according to one prior study (Buitenhuis et al., 1999), but subsaturating for POC production according to a more recent study (Bach et al., 2013). The experimental variability noted might have accentuated a variability among strains in the affinity of *E. huxleyi* for photosynthetic carbon uptake. Bach et al. (2013) also reported that growth rate was saturated at lower dissolved CO₂ levels than POC production. A similar increase in POC quota in response to high CO₂ has been reported in *Calcidiscus quadripforatus* strain RCC 1168 to correlate with the production of transparent exopolysaccharides (TEPs) (Diner et al., 2015), and so we suspect that the increase in POC per cell – at least in CHC342 – might correspond partly to increased TEP production under high CO₂ and low pH.

As expected, PIC quotas varied among strains. CHC342, the strain showing the greatest degree of over-calcification, showed the highest PIC quota. Strain CHC440, the strain showing the coccoliths with the least percentage covering of the central area by the inner tube and the most delicate distal shield rim elements, showed the lowest PIC quota. However, the PIC quotas of CHC352, CHC360, and CHC428 were not different. The numbers of detached coccoliths per cell were similar among those three strains, but coccoliths produced by CHC428 were slightly larger, partly explaining this result. The PIC / POC ratio also did not show consistent differences among morphotypes.

PIC / POC ratios decreased in all strains and all treatments, similar to what has been reported for most of the strains used in most of the previous studies (reviewed in Meyer and Riebesell, 2015). However, in future studies it will be important to understand how TEP production impacts POC and PIC / POC ratios and responds to high CO₂ and low pH, as has been shown in *Calcidiscus* (Diner et al., 2015). The effect of high CO₂ and low pH on calcification (PIC quota and PIC production) was variable among strains, with no clear pattern related to origin or calcification, and none of these modest effects were significant except the increase in PIC quota in CHC342, the most heavily calcified strain. While calcification rate appears to be sensitive to high CO₂ and low pH in most studies and strains of *E. huxleyi* (Meyer and Riebesell, 2015) despite periods of acclimation,

or even adaptation over hundreds of generations (Lohbeck et al., 2012), all of the strains tested here appear to be more similar in this aspect to strains found to exhibit calcification that is relatively resistant to high CO₂ and low pH (Langer et al., 2009). We did not see the dramatic loss of calcification (almost all cells were calcified in all strains and treatments) that was reported, for example, in a B/C morphotype from the Southern Ocean in response to high CO₂ and low pH (Müller et al., 2015a).

We caution that the changes in alkalinity suggested that both strain CHC342 and strain CHC440 may have had an approximately 2-fold higher PIC quota than what was directly measured under the control CO₂ and pH condition. This could have occurred if the acidification of total particulate carbon samples did not effectively dissolve all calcium carbonate in these strains. This is surprising, as the geochemical analysis service that performed POC and PIC measurements followed a standard protocol recommended for both plankton samples and carbonate-rich soil samples (Harris et al., 2001; Lorrain et al., 2003) that has been previously used for measuring PIC and POC quotas in *E. huxleyi* (Zondervan et al., 2002; Sciandra et al., 2003). We speculate that perhaps the coccoliths from these strains differ from other strains in organic content in some way that makes them more resistant to dissolution. For example, recent comparisons have shown that the content and composition of coccolith-associated polysaccharides varies among *E. huxleyi* strains (Lee et al., 2016). However, we are not aware of such an effect being reported in the literature. In any case, a possible underestimation of PIC quotas in strains CHC342 and CHC440 under the control CO₂ and pH condition would mean that the POC quota was overestimated under that condition, accentuating the increase in POC by high CO₂ and low pH. Most importantly, it implies these strains may not have experienced an increase in PIC quota in response to high CO₂ and low pH, but instead PIC quota might have actually been either maintained or decreased.

The function of coccoliths is still not certain. However, calcification is costly. It is not immediately clear if the proposed role of calcification to alleviate Ca²⁺ toxicity could cause the selection of over-calcified coccoliths in the high-CO₂-low-pH upwelling waters, as the differences in Ca²⁺ concentrations are vanishingly small compared to the levels at which calcification was observed to show this benefit in the lab (Müller et al., 2015b). Likewise, a possible physiological role of calcification as a carbon-concentrating mechanism to support photosynthesis in low-CO₂ waters is not supported by the current balance of evidence in published literature for *E. huxleyi* (Trimborn et al., 2007) as reviewed in Monteiro et al. (2016). In any case, such an explanation could not explain why highly calcified cells would be selected for in high-CO₂ waters. Most evidence suggests calcification may serve protective or defensive functions (Monteiro et al., 2016), in which case not only the rate of calcification but also the form and quality of the coccoliths would be important. Thus we

also considered responses in coccolith morphology when analyzing potential adaptation.

Both microscopic and flow cytometric measures indicated that coccolith morphology was not more resistant to high-CO₂–low-pH conditions in the R/over-calcified strains isolated from naturally high-CO₂–low-pH upwellings than in the A morphotype strains isolated from far offshore waters in equilibrium with the atmosphere that are not known to experience natural high-CO₂–low-pH episodes. The increase in the percentages of malformed or incomplete coccoliths in response to high CO₂ and low pH was most pronounced in the R/over-calcified morphotypes, although these percentages remained low in all strains and both treatments compared to other studies. In other *E. huxleyi* morphotypes, the thickness of the tube around the coccolith central area is reported to decrease modestly under acidification conditions (Bach et al., 2012; Young et al., 2014), and a similar effect was seen in the two A morphotype strains here. In our study, this effect was most pronounced, resulting in a highly eroded appearance, in the most heavily over-calcified R strains in which the tube overgrows the central area. Coccoliths are formed in intracellular compartments, and the extracellular Ω_{Ca} remained > 1 in the experiments, so this must be due to effects on the formation of coccoliths, not erosion after coccolith secretion. This also shows that the degree of covering of the central area in these types depends on condition in the R morphotype; however, the principal morphotype classification of each of the five strains did not change, as expected if morphotype is genetically determined (Young and Westbroek, 1991). The disappearance of the underlying central area (hollow coccoliths) reported in one study (Lefebvre et al., 2012) was not observed here. The morphological observations using SEM were supported by flow cytometric results, which also showed changes in the relative depolarization of forward scatter light of both whole coccospheres and detached coccoliths.

The observation that the morphology and quality of coccoliths of moderately calcified A morphotype strains were comparatively little affected while R/over-calcified forms were strongly affected does not appear consistent with the hypothesis that over-calcification of distal shield elements in the *E. huxleyi* present in naturally acidified high-CO₂ water serves to compensate for high-CO₂–low-pH effects on coccoliths. Some other factor must select for the R/over-calcified morphotype in the coastal zone of Chile. An A morphotype (A*) exhibiting partial and irregular extension of inner tube elements over the central area (but not closure of spaces between distal shield radial elements) was dominant in the Benguela upwelling zone (not the more extreme R/over-calcified types) (Henderiks et al., 2012), while the A_{CC} type, although rare off the coast of Chile, was dominant in the northeastern Atlantic (Bay of Biscay) in winter (Smith et al., 2012). It is interesting to speculate that high-productivity conditions in eastern boundary coastal waters promote persistently higher abundances of grazers or phy-

topathogenic bacteria, against which the over-calcified coccoliths might provide better defense.

The lack of evidence for regional-scale local adaptation (either in terms of growth or morphology) to short-term high-CO₂–low-pH conditions in *E. huxleyi* populations that are naturally exposed to pulses of naturally high-CO₂–low-pH upwelling conditions, contrasts with the recent findings showing adaptation to OA in estuarine habitats in invertebrates and coralline algae (Padilla-Gamiño et al., 2016; Gaitán-Espitia et al., 2017; Vargas et al., 2017), including the neritic but holoplanktonic copepod *Acartia tonsa* (Vargas et al., 2017). However, among *E. huxleyi* there is variability in response to high CO₂ and low pH (Riebesell et al., 2000; Iglesias-Rodriguez et al., 2008; Langer et al., 2009; Meyer and Riebesell, 2015) that appears to correlate with morphotype and origin at least in one study (Müller et al., 2015a). This variability may already have been subject to selection. In that case, perhaps it is appropriate to consider that the present study documented a similar resistance of offshore eastern South Pacific A morphotype strains to that of coastal strains from high-CO₂–low-pH waters. Although the offshore populations should be exposed less to high-CO₂–low-pH conditions, they might experience such conditions occasionally: intra-thermocline eddies, subsurface lenses between approximately 100 and 500 m depth, have recently been documented to transport subsurface waters low in dissolved O₂ in an offshore direction in the eastern South Pacific (Andrade et al., 2014; Combes et al., 2015). These eddies would also be expected to be high in CO₂ and low in pH, and intrusions of such water might affect organisms at the base of the euphotic zone. Such processes would still result in lower CO₂ exposure than the exposure to high CO₂ and low pH occurring at the coast. Perhaps the nearshore *E. huxleyi* populations, despite being exposed more frequently and more intensely to high-CO₂–low-pH conditions, have already reached some limit that prevents adaptation to further increases in CO₂, which limit the negative effects of these conditions on growth rate, calcification, and coccolithogenesis. Overall, the observation of consistent declines in growth rates, PIC quotas, and PIC / POC ratios, even in genotypes that naturally are exposed to high-CO₂–low-pH conditions, supports the prediction that PIC-associated POC export may decline under future OA conditions, potentially weakening the biological pump (Hofmann and Schellnhuber, 2009).

Data availability. All data are available from the corresponding author upon request. The scanning electron micrograph image datasets can be found at <https://doi.org/10.5281/zenodo.1194799> (von Dassow et al., 2018).

The Supplement related to this article is available online at <https://doi.org/10.5194/bg-15-1515-2018-supplement>.

Author contributions. PvD led the study, carried out sampling in field surveys, performed flow cytometric isolation of *E. huxleyi* strains, carried out statistical analysis of experimental data, supervised processing of samples with flow cytometry and electron microscopy, and wrote the paper. FDR conducted characterization of coccolithophore communities and *E. huxleyi* morphotype composition, analyzed the relationships of coccolithophore communities and *E. huxleyi* morphotypes to environmental parameters, assisted with part of the high-CO₂-low-pH experiments in the Calfuco Marine Laboratory, and helped prepare the first draft of the paper and figures. EMB participated in field studies in 2012, helped with classification of *E. huxleyi* morphotypes, and trained and supervised FDR in coccolithophore taxonomic classification. JDGE led experimental work in the Calfuco laboratory and provided key comments and editing of the paper. SR provided insights into interpretation of results and edited a draft of the paper. DMF helped plan and perform experiments in the Calfuco lab. UJ assisted with initial plans and later interpretations. RT performed chemical analysis on seawater samples and helped set up the Calfuco Marine Laboratory experiments.

Competing interests. The authors declare they have no conflicts of interest.

Acknowledgements. This work was supported by the Comisión Nacional de Investigación Científica y Tecnológica of the Chilean Ministry of Education (FONDECYT grants 1110575 and 1141106, and grant CONICYT USA 20120014 to Peter von Dassow, a doctoral fellowship CONICYT-PCHA/Doctorado Nacional/2013–21130158 to Francisco Díaz-Rosas, FONDECYT postdoc grant 312004 to Daniella Mella-Flores, and FONDEQUIP EQM130267 for the purchase of the Influx cell sorter), by the Iniciativa Científica Milenio of the Chilean Ministry of Economy through the Instituto Milenio de Oceanografía de Chile (grant IC 120019), by the ASSEMBLE program (grant 227799; El Mahdi Bendif), and by International Research Network “Diversity, Evolution and Biotechnology of Marine Algae” (GDRI no. 0803) of the Centre National de Recherche Scientifique (Peter von Dassow). The authors thank Jorge Navarro for access to the Calfuco Marine Laboratory, Veronica Flores for assisting with SEM analysis, and Jessica Beltrán for work as lab manager of the Santiago lab.

Edited by: Lennart de Nooijer

Reviewed by: Marius N. Müller and one anonymous referee

References

- Andrade, I., Hormazabal, S., and Combes, V.: Intrathermocline eddies at the Juan Fernández Archipelago, southeastern Pacific Ocean, *Lat. Am. J. Aquat. Res.*, 42, 888–906, <https://doi.org/10.3856/vol42-issue4-fulltext-14>, 2014.
- Armstrong, R. A., Lee, C., Hedges, J. I., Honjo, S., and Wakeham, S. G.: A new, mechanistic model for organic carbon fluxes in the ocean based on the quantitative association of POC with ballast minerals, *Deep-Sea Res. Pt. II*, 49, 219–236, [https://doi.org/10.1016/S0967-0645\(01\)00101-1](https://doi.org/10.1016/S0967-0645(01)00101-1), 2002.
- Bach, L. T., Bauke, C., Meier, K. J. S., Riebesell, U., and Schulz, K. G.: Influence of changing carbonate chemistry on morphology and weight of coccoliths formed by *Emiliania huxleyi*, *Bio-geosciences*, 9, 3449–3463, <https://doi.org/10.5194/bg-9-3449-2012>, 2012.
- Bach, L. T., Mackinder, L. C. M., Schulz, K. G., Wheeler, G., Schroeder, D. C., Brownlee, C., and Riebesell, U.: Dissecting the impact of CO₂ and pH on the mechanisms of photosynthesis and calcification in the coccolithophore *Emiliania huxleyi*, *New Phytol.*, 199, 121–134, 2013.
- Baith, K., Lindsay, R., Fu, G., and McClain, C. R.: SeaDAS, a data analysis system for ocean-color satellite sensors, *Eos T. Am. Geophys. Un.*, 82, 202–202, <https://doi.org/10.1029/01EO00109>, 2001.
- Beaufort, L., Probert, I., de Garidel-Thoron, T., Bendif, E. M., Ruiz-Pino, D., Metzl, N., Goyet, C., Buchet, N., Coupel, P., Grelaud, M., Rost, B., Rickaby, R. E. M., and de Vargas, C.: Sensitivity of coccolithophores to carbonate chemistry and ocean acidification, *Nature*, 476, 80–83, <https://doi.org/10.1038/nature10295>, 2011.
- Bendif, E. M., Probert, I., Díaz-Rosas, F., Thomas, D., van den Engh, G., Young, J. R., and von Dassow, P.: Recent reticulate evolution in the ecologically dominant lineage of coccolithophores, *Front. Microbiol.*, 7, 784, <https://doi.org/10.3389/fmicb.2016.00784>, 2016.
- Buitenhuis, E. T., De Baar, H. J. W., and Veldhuis, M. J. W.: Photosynthesis and calcification by *Emiliania huxleyi* (Prymnesiophyceae) as a function of inorganic carbon species, *J. Phycol.*, 35, 949–959, 1999.
- Combes, V., Hormazabal, S., and Di Lorenzo, E.: Interannual variability of the subsurface eddy field in the Southeast Pacific, *J. Geophys. Res.-Oceans*, 120, 4907–4924, <https://doi.org/10.1002/2014JC010265>, 2015.
- Cubillos, J. C., Wright, S. W., Nash, G., De Salas, M. F., Griffiths, B., Tilbrook, B., Poisson, A., and Hallegraeff, G. M.: Calcification morphotypes of the coccolithophorid *Emiliania huxleyi* in the Southern Ocean: changes in 2001 to 2006 compared to historical data, *Mar. Ecol.-Prog. Ser.*, 348, 47–54, <https://doi.org/10.3354/meps07058>, 2007.
- Dickson, A. G.: Standards for ocean measurements, *Oceanography*, 23, 34–47, <https://doi.org/10.5670/oceanog.2010.22>, 2010.
- Dickson, A. G. and Millero, F. J.: A comparison of the equilibrium constants for the dissociation of carbonic acid in seawater media, *Deep-Sea Res.*, 34, 1733–1743, [https://doi.org/10.1016/0198-0149\(87\)90021-5](https://doi.org/10.1016/0198-0149(87)90021-5), 1987.
- Dickson, A. G., Sabine, C. L., and Christian, J. R. (Eds.): Guide to Best Practices for Ocean CO₂ Measurements, PICES Special Publication 3, Victoria, BC, Canada, 2007.
- Diner, R. E., Benner, I., Passow, U., Komada, T., Carpenter, E. J., and Stillman, J. H.: Negative effects of ocean acidification on calcification vary within the coccolithophore genus *Calcidiscus*, *Mar. Biol.*, 162, 1287–1305, <https://doi.org/10.1007/s00227-015-2669-x>, 2015.
- DOE: Handbook of methods for the analysis of the various parameters of the carbon dioxide system in sea water, edited by: Dickson, A. G. and Goyet, C., ORNL/CDIAC-74, available at: http://cdiac.ornl.gov/oceans/DOE_94.pdf (last access: 29 August 2013), 1994.

- Engel, A., Zondervan, I., Aerts, K., Beaufort, L., Benthien, A., Chou, L., Delille, B., Gattuso, J.-P., Harlay, J., Heemann, C., Hoffmann, L., Jacquet, S., Nejstgaard, J., Pizay, M.-D., Rochelle-Newall, E., Schneider, U., Terbruggen, A., and Riebesell, U.: Testing the direct effect of CO₂ concentration on a bloom of the coccolithophorid *Emiliana huxleyi* in mesocosm experiments, *Limnol. Oceanogr.*, 50, 493–507, 2005.
- Frankignoulle, M., Canon, C., and Gattuso, J.: Marine calcification as a source of carbon dioxide: Positive feedback of increasing atmospheric CO₂, *Limnol. Oceanogr.*, 39, 458–462, 1994.
- Friederich, G. E., Ledesma, J., Ulloa, O., and Chavez, F. P.: Air–sea carbon dioxide fluxes in the coastal south-eastern tropical Pacific, *Prog. Oceanogr.*, 79, 156–166, <https://doi.org/10.1016/j.pocean.2008.10.001>, 2008.
- Gaitán-Espitia, J. D., Villanueva, P. A., Lopez, J., Torres, R., Navarro, J. M., and Bacigalupe, L. D.: Spatio-temporal environmental variation mediates geographical differences in phenotypic responses to ocean acidification, *Biol. Letters*, 13, 20160865, <https://doi.org/10.1098/rsbl.2016.0865>, 2017.
- Hagino, K., Bendif, E. M., Young, J. R., Kogame, K., Probert, I., Takano, Y., Horiguchi, T., de Vargas, C., and Okada, H.: New evidence for morphological and genetic variation in the cosmopolitan coccolithophore *Emiliana huxleyi* (Prymnesiophyceae) from the *cox1b-atp4* genes, *J. Phycol.*, 47, 1164–1176, <https://doi.org/10.1111/j.1529-8817.2011.01053.x>, 2011.
- Harris, D., Horváth, W. R., and van Kessel, C.: Acid fumigation of soils to remove carbonates prior to total organic carbon or carbon-13 isotopic analysis, *Soil Sci. Soc. Am. J.*, 65, 1853–1856, 2001.
- Henderiks, J., Winter, A., Elbrächter, M., Feistel, R., Van Der Plas, A., Nausch, G., and Barlow, R.: Environmental controls on *Emiliana huxleyi* morphotypes in the Benguela coastal upwelling system (SE Atlantic), *Mar. Ecol.-Prog. Ser.*, 448, 51–66, <https://doi.org/10.3354/meps09535>, 2012.
- Heraldsson, C., Anderson, L. G., Hassellöv, M., Hulth, S., and Olsson, K.: Rapid, high-precision potentiometric titration of alkalinity in ocean and sediment pore waters, *Deep-Sea Res. Pt. I*, 44, 2031–2044, [https://doi.org/10.1016/S0967-0637\(97\)00088-5](https://doi.org/10.1016/S0967-0637(97)00088-5), 1997.
- Hofmann, M. and Schellnhuber, H.-J.: Oceanic acidification affects marine carbon pump and triggers extended marine oxygen holes, *P. Natl. Acad. Sci. USA*, 106, 3017–3022, <https://doi.org/10.1073/pnas.0813384106>, 2009.
- Hofmann, G. E., Smith, J. E., Johnson, K. S., Send, U., Levin, L. A., Micheli, F., Paytan, A., Price, N. N., Peterson, B., Takeshita, Y., Matson, P. G., de Crook, E., Kroeker, K. J., Gambi, M. C., Rivest, E. B., Frieder, C. A., Yu, P. C., and Martz, T. R.: High-frequency dynamics of ocean pH: A multi-ecosystem comparison, *PLoS One*, 6, e28983, <https://doi.org/10.1371/journal.pone.0028983>, 2011.
- Iglesias-Rodríguez, M. D., Brown, C. W., Doney, S. C., Kleypas, J., Kolber, D., Kolber, Z., Hayes, P. K., and Falkowski, P. G.: Representing key phytoplankton functional groups in ocean carbon cycle models: Coccolithophorids, *Global Biogeochem. Cy.*, 16, 47-1–47-20, <https://doi.org/10.1029/2001GB001454>, 2002.
- Iglesias-Rodríguez, M. D., Halloran, P. R., Rickaby, R. E. M., Hall, I. R., Colmenero-Hidalgo, E., Gittins, J. R., Green, D. R. H., Tyrrell, T., Gibbs, S. J., von Dassow, P., Rehm, E., Armbrust, E. V., and Boessenkool, K. P.: Phytoplankton calcification in a high-CO₂ world, *Science*, 320, 336–340, <https://doi.org/10.1126/science.1154122>, 2008.
- Jin, P., Ding, J., Xing, T., Riebesell, U., and Gao, K.: High levels of solar radiation offset impacts of ocean acidification on calcifying and non-calcifying strains of *Emiliana huxleyi*, *Mar. Ecol.-Prog. Ser.*, 568, 47–58, 2017.
- Keller, M. D., Selvin, R. C., Claus, W., and Guillard, R. R.: Media for the culture of oceanic ultraphytoplankton, *J. Phycol.*, 23, 633–638, 1987.
- Krueger-Hadfield, S. A., Balestreri, C., Schroeder, J., Highfield, A., Helaouët, P., Allum, J., Moate, R., Lohbeck, K. T., Miller, P. I., Riebesell, U., Reusch, T. B. H., Rickaby, R. E. M., Young, J., Hallegraeff, G., Brownlee, C., and Schroeder, D. C.: Genotyping an *Emiliana huxleyi* (prymnesiophyceae) bloom event in the North Sea reveals evidence of asexual reproduction, *Biogeosciences*, 11, 5215–5234, <https://doi.org/10.5194/bg-11-5215-2014>, 2014.
- Langer, G., Nehrke, G., Probert, I., Ly, J., and Ziveri, P.: Strain-specific responses of *Emiliana huxleyi* to changing seawater carbonate chemistry, *Biogeosciences*, 6, 2637–2646, <https://doi.org/10.5194/bg-6-2637-2009>, 2009.
- Lee, R. B. Y., Mavridou, D. A. I., Papadakos, G., McClelland, H. L. O., and Rickaby, R. E. M.: The uronic acid content of coccolith-associated polysaccharides provides insight into coccolithogenesis and past climate, *Nat. Commun.*, 7, 13144, <https://doi.org/10.1038/ncomms13144>, 2016.
- Lefebvre, S. C., Benner, I., Stillman, J. H., Parker, A. E., Drake, M. K., Rossignol, P. E., Okimura, K. M., Komada, T., and Carpenter, E. J.: Nitrogen source and *p*CO₂ synergistically affect carbon allocation, growth and morphology of the coccolithophore *Emiliana huxleyi*: Potential implications of ocean acidification for the carbon cycle, *Glob. Change Biol.*, 18, 493–503, <https://doi.org/10.1111/j.1365-2486.2011.02575.x>, 2012.
- Litchman, E., de Tezanos Pinto, P., Edwards, K. F., Klausmeier, C. A., Kremer, C. T., and Thomas, M. K.: Global biogeochemical impacts of phytoplankton: A trait-based perspective, *J. Ecol.*, 103, 1384–1396, <https://doi.org/10.1111/1365-2745.12438>, 2015.
- Lohbeck, K. T., Riebesell, U., and Reusch, T. B. H.: Adaptive evolution of a key phytoplankton species to ocean acidification, *Nat. Geosci.*, 5, 917–917, <https://doi.org/10.1038/ngeo1637>, 2012.
- Lorrain, A., Savoye, N., Chauvaud, L., Paulet, Y.-M., and Naulet, N.: Decarbonation and preservation method for the analysis of organic C and N contents and stable isotope ratios of low-carbonate suspended particulate material, *Anal. Chim. Acta*, 491, 125–133, [https://doi.org/10.1016/S0003-2670\(03\)00815-8](https://doi.org/10.1016/S0003-2670(03)00815-8), 2003.
- McDonald, M. J., Rice, D. P., and Desai, M. M.: Sex speeds adaptation by altering the dynamics of molecular evolution, *Nature*, 531, 233–236, <https://doi.org/10.1038/nature17143>, 2016.
- Mehrbach, C., Culbertson, C. H., Hawley, J. E., and Pytkowicz, R. M.: Measurement of the apparent dissociation constants of carbonic acid in seawater at atmospheric pressure, *Limnol. Oceanogr.*, 18, 897–907, 1973.
- Meyer, J. and Riebesell, U.: Reviews and Syntheses: Responses of coccolithophores to ocean acidification: a meta-analysis, *Biogeosciences*, 12, 1671–1682, <https://doi.org/10.5194/bg-12-1671-2015>, 2015.

- Monteiro, F. M., Bach, L. T., Brownlee, C., Bown, P., Rickaby, R. E. M., Poulton, A. J., Tyrrell, T., Beaufort, L., Dutkiewicz, S., Gibbs, S., Gutowska, M. A., Lee, R., Riebesell, U., Young, J., and Ridgwell, A.: Why marine phytoplankton calcify, *Sci. Adv.*, 2, e1501822–e1501822, <https://doi.org/10.1126/sciadv.1501822>, 2016.
- Müller, M. N., Trull, T. W., and Hallegraeff, G. M.: Differing responses of three Southern Ocean *Emiliana huxleyi* ecotypes to changing seawater carbonate chemistry, *Mar. Ecol.-Prog. Ser.*, 531, 81–90, 2015a.
- Müller, M. N., Barcelos e Ramos, J., Schulz, K. G., Riebesell, U., Kaźmierczak, J., Gallo, F., Mackinder, L., Li, Y., Nesterenko, P. N., Trull, T. W., and Hallegraeff, G. M.: Phytoplankton calcification as an effective mechanism to alleviate cellular calcium poisoning, *Biogeosciences*, 12, 6493–6501, <https://doi.org/10.5194/bg-12-6493-2015>, 2015b.
- Müller, M. N., Trull, T. W., and Hallegraeff, G. M.: Independence of nutrient limitation and carbon dioxide impacts on the Southern Ocean coccolithophore *Emiliana huxleyi*, *ISME J.*, 11, 1777–1787, <https://doi.org/10.1038/ismej.2017.53>, 2017.
- NASA Goddard Space Flight Center, Ocean Ecology Laboratory, and Ocean Biology Processing Group: Moderate-resolution Imaging Spectroradiometer (MODIS) Aqua Ocean Color Data, 2014 Reprocessing, NASA OB.DAAC, Greenbelt, MD, USA, https://doi.org/10.5067/AQUA/MODIS_OC.2014.0 (last access: 23 December 2015), 2014.
- Olson, M. B., Wuori, T. A., Love, B. A., and Strom, S. L.: Ocean acidification effects on haploid and diploid *Emiliana huxleyi* strains: Why changes in cell size matter, *J. Exp. Mar. Biol. Ecol.*, 488, 72–82, <https://doi.org/10.1016/j.jembe.2016.12.008>, 2017.
- Orr, J. C., Fabry, V. J., Aumont, O., Bopp, L., Doney, S. C., Feely, R. A., Gnanadesikan, A., Gruber, N., Ishida, A., Joos, F., Key, R. M., Lindsay, K., Maier-Reimer, E., Matear, R., Monfray, P., Mouchet, A., Najjar, R. G., Plattner, G.-K., Rodgers, K. B., Sabine, C. L., Sarmiento, J. L., Schlitzer, R., Slater, R. D., Totterdell, I. J., Weirig, M.-F., Yamanaka, Y., and Yool, A.: Anthropogenic ocean acidification over the twenty-first century and its impact on calcifying organisms, *Nature*, 437, 681–686, <https://doi.org/10.1038/nature04095>, 2005.
- Paasche, E.: A review of the coccolithophorid *Emiliana huxleyi* (Prymnesiophyceae) with particular reference to growth, coccolith formation, and calcification-photosynthesis interactions, *Phycologia*, 40, 503–529, <https://doi.org/10.2216/i0031-8884-40-6-503.1>, 2002.
- Padilla-Gamiño, J. L., Gaitán-Espitia, J. D., Kelly, M. W., and Hofmann, G. E.: Physiological plasticity and local adaptation to elevated $p\text{CO}_2$ in calcareous algae?: an ontogenetic and geographic approach, *Evol. Appl.*, 9, 1043–1053, <https://doi.org/10.1111/eva.12411>, 2016.
- Pierrot, D., Lewis, D. E., and Wallace, D. W. R.: CO2SYS. EXE – MS excel program developed for CO2 system calculations, <http://cdiac.ornl.gov/ftp/co2sys> (last access: 8 November 2014), 2006.
- Poulton, A. J., Young, J. R., Bates, N. R., and Balch, W. M.: Biometry of detached *Emiliana huxleyi* coccoliths along the Patagonian Shelf, *Mar. Ecol.-Prog. Ser.*, 443, 1–17, <https://doi.org/10.3354/meps09445>, 2011.
- Richier, S., Fiorini, S., Kerros, M. E., von Dassow, P., and Gattuso, J. P.: Response of the calcifying coccolithophore *Emiliana huxleyi* to low pH/high $p\text{CO}_2$: From physiology to molecular level, *Mar. Biol.*, 158, 551–560, 2011.
- Riebesell, U., Zondervan, I., Rost, B., Tortell, P. D., Zeebe, R. E., and Morel, F. M.: Reduced calcification of marine plankton in response to increased atmospheric CO_2 , *Nature*, 407, 364–367, <https://doi.org/10.1038/35030078>, 2000.
- Riebesell, U., Bach, L. T., Bellerby, R. G. J., Monsalve, J. R. B., Boxhammer, T., Czerny, J., Larsen, A., Ludwig, A., and Schulz, K. G.: Competitive fitness of a predominant pelagic calcifier impaired by ocean acidification, *Nat. Geosci.*, 10, 19–23, <https://doi.org/10.1038/NNGEO2854>, 2017.
- Rokitta, S. D. and Rost, B.: Effects of CO_2 and their modulation by light in the life-cycle stages of the coccolithophore *Emiliana huxleyi*, *Limnol. Oceanogr.*, 57, 607–618, <https://doi.org/10.4319/lo.2012.57.2.0607>, 2012.
- Rosas-Navarro, A., Langer, G., and Ziveri, P.: Temperature affects the morphology and calcification of *Emiliana huxleyi* strains, *Biogeosciences*, 13, 2913–2926, <https://doi.org/10.5194/bg-13-2913-2016>, 2016.
- Sabine, C. L., Feely, R. A., Gruber, N., Key, R. M., Lee, K., Bullister, J. L., Wanninkhof, R., Wong, C. S., Wallace, D. W. R., Tilbrook, B., Millero, F. J., Peng, T.-H., Kozyr, A., Ono, T., and Rios, A. F.: The Oceanic Sink for anthropogenic CO_2 , *Science*, 305, 367–371, <https://doi.org/10.1126/science.1097403>, 2004.
- Sanders, R., Morris, P. J., Poulton, A. J., Stinchcombe, M. C., Charalampopoulou, A., Lucas, M. I., and Thomalla, S. J.: Does a ballast effect occur in the surface ocean?, *Geophys. Res. Lett.*, 37, 1–5, <https://doi.org/10.1029/2010GL042574>, 2010.
- Schlüter, L., Lohbeck, K. T., Gröger, J. P., Riebesell, U., and Reusch, T. B. H.: Long-term dynamics of adaptive evolution in a globally important phytoplankton species to ocean acidification, *Sci. Adv.*, 2, e1501660–e1501660, <https://doi.org/10.1126/sciadv.1501660>, 2016.
- Sciandra, A., Harlay, J., Lefèvre, D., Lemée, R., Rimmelin, P., Denis, M., and Gattuso, J.-P.: Response of coccolithophorid *Emiliana huxleyi* to elevated partial pressure of CO_2 under nitrogen limitation, *Mar. Ecol.-Prog. Ser.*, 261, 111–122, 2003.
- Shi, D., Xu, Y., and Morel, F. M. M.: Effects of the pH/ $p\text{CO}_2$ control method on medium chemistry and phytoplankton growth, *Biogeosciences*, 6, 1199–1207, <https://doi.org/10.5194/bg-6-1199-2009>, 2009.
- Smith, H. E. K., Tyrrell, T., Charalampopoulou, A., Dumousseaud, C., Legge, O. J., Birchenough, S., Pettit, L. R., Garley, R., Hartman, S. E., Hartman, M. C., Sagoo, N., Daniels, C. J., Achterberg, E. P., and Hydes, D. J.: Predominance of heavily calcified coccolithophores at low CaCO_3 saturation during winter in the Bay of Biscay, *P. Natl. Acad. Sci. USA*, 109, 8845–8849, <https://doi.org/10.1073/pnas.1117508109>, 2012.
- Thiel, M., Macaya, E. C., Acuña, E., Arntz, W. E., Bastias, H., Brokordt, K., Camus, P. A., Castilla, J. C., Castro, L. R., Cortés, M., Dumont, C. P., Escribano, R., Fernández, M., Gajardo, J. A., Gaymer, C. F., Gomez, I., González, A. E., González, H. E., Haye, P. A., Illanes, J. E., Iriarte, J. L., Lancellotti, D. A., Luna-Jorquera, G., Luxoro, C., Manriquez, P. H., Marín, V., Muñoz, P., Navarretes, S. A., Perez, E., Poulin, E., Sellanes, J., Sepúlveda, H. H., Stotz, W., Tala, F., Thomas, A., Vargas, C. A., Vasquez, J. A., and Vega, J. M. A.: The Humboldt current system of northern and central Chile Oceanographic processes, ecological interactions and

- socioeconomic feedback, *Oceanogr. Mar. Biol.*, 45, 195–344, <https://doi.org/10.1201/9781420050943>, 2007.
- Torres, R., Turner, D. R., Silva, N., and Rutllant, J.: High short-term variability of CO₂ fluxes during an upwelling event off the Chilean coast at 30° S, *Deep-Sea Res. Pt. I*, 46, 1161–1179, 1999.
- Torres, R., Turner, D. R., Silva, N., and Rutllant, J.: High short-term variability of CO₂ fluxes during an upwelling event off the Chilean coast at 30° S, *Deep Sea Res. Pt. I*, 46, 1161–1179, 1999.
- Torres, R., Manriquez, P. H., Duarte, C., Navarro, J. M., Lagos, N. A., Vargas, C. A., and Lardies, M. A.: Evaluation of a semi-automatic system for long-term seawater carbonate chemistry manipulation, *Rev. Chil. Hist. Nat.*, 86, 443–451, <https://doi.org/10.4067/S0716-078X2013000400006>, 2013.
- Trimborn, S., Langer, G., and Rost, B.: Effect of varying calcium concentrations and light intensities on calcification and photosynthesis in *Emiliana huxleyi*, *Limnol. Oceanogr.*, 52, 2285–2293, 2007.
- Vargas, C. A., Lagos, N. A., Lardies, M. A., Duarte, C., Manríquez, P. H., Aguilera, V. M., Broitman, B., Widdicombe, S., and Dupont, S.: Species-specific responses to ocean acidification should account for local adaptation and adaptive plasticity, *Nat. Ecol. Evol.*, 1, 84, <https://doi.org/10.1038/s41559-017-0084>, 2017.
- Von Dassow, P., Van Den Engh, G., Iglesias-Rodriguez, D., and Gittins, J. R.: Calcification state of coccolithophores can be assessed by light scatter depolarization measurements with flow cytometry, *J. Plankton Res.*, 34, 1011–1027, <https://doi.org/10.1093/plankt/fbs061>, 2012.
- Von Dassow, P., Diaz-Rosas, F., Bendif, E. M., Gaitan-Espitia, J.-D., Mella-Flores, D., Rokitta, S., John, U., and Torres, R.: Scanning electron microscopy datasets – *Emiliana huxleyi* strains from naturally high and low CO₂ waters responding to high and low CO₂ in the lab [Dataset], Zenodo, <https://doi.org/10.5281/zenodo.1194799>, 2018.
- Young, J. R. and Westbroek, P.: Genotypic variation in the coccolithophorid species *Emiliana huxleyi*, *Mar. Micropaleontol.*, 18, 5–23, [https://doi.org/10.1016/0377-8398\(91\)90004-P](https://doi.org/10.1016/0377-8398(91)90004-P), 1991.
- Young, J. R., Geisen, M., Cros, L., Kleijne, A., Sprengel, C., Probert, I., and Østergaard, J. B.: A guide to extant coccolithophore taxonomy, *J. Nannoplankt. Res.*, 1, 1–125, 2003.
- Young, J. R., Poulton, A. J., and Tyrrell, T.: Morphology of *Emiliana huxleyi* coccoliths on the northwestern European shelf – is there an influence of carbonate chemistry?, *Biogeosciences*, 11, 4771–4782, <https://doi.org/10.5194/bg-11-4771-2014>, 2014.
- Zondervan, I., Rost, B., and Riebesell, U.: Effect of CO₂ concentration on the PIC / POC ratio in the coccolithophore *Emiliana huxleyi* grown under light-limiting conditions and different daylengths, *J. Exp. Mar. Biol. Ecol.*, 272, 55–70, 2002.